4th International Conference on Nanotek & Expo
December 01-03, 2014, San Francisco, USA

Construction, Functionalization, and Organization of Dendrimer with Conjugated Backbones

Masatoshi Kozaki*, Shuichi Suzuki, Keiji Okada

Graduate School of Science, Osaka City University, Osaka 558-8585 Japan

E-mail: kozaki@sci.osaka-cu.ac.jp

Element-Block Polymers

科研費 KAKENHI

Top-down and Bottom-up Approach to Nano-scale Architectures

Moore's Low

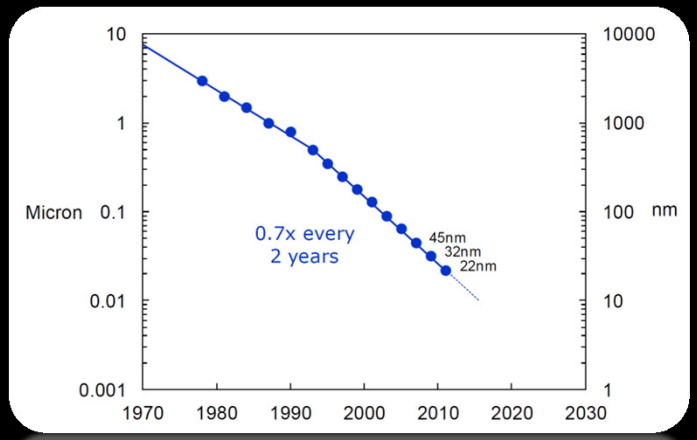

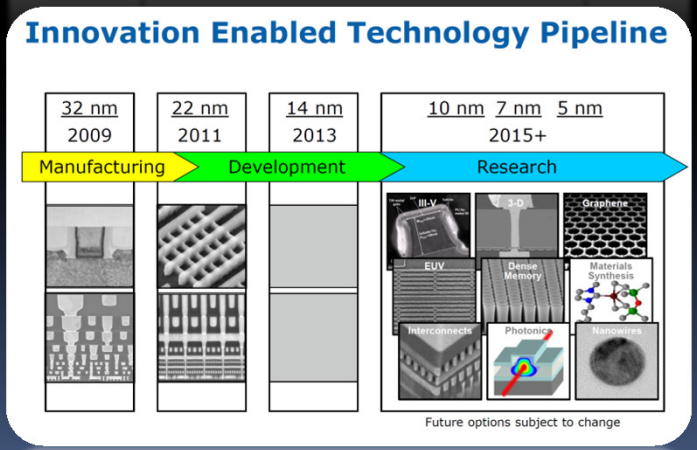

Top-down

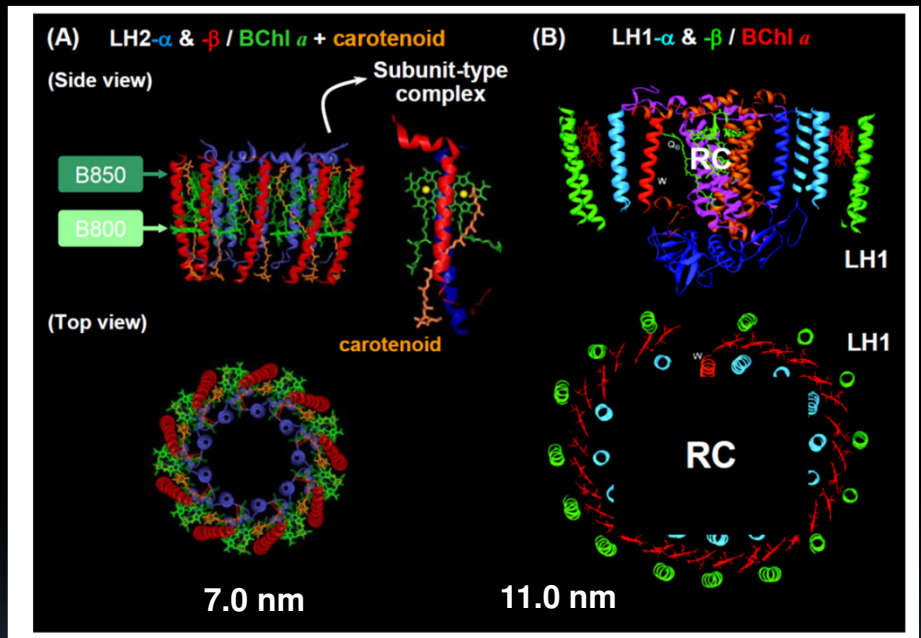

Figure 2. 3-D crystal structures of **(A)** LH2 complex and its subunit-type complex from *Rps. acidophila* strain 10050 (*18*) and **(B)** LH1-RC core complex from *Rps. palustris* (*19*).

Bottom-up

The Concept of the Stepwise Approach to Nano-scale Architectures

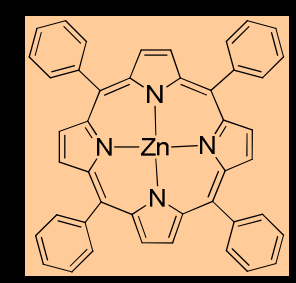

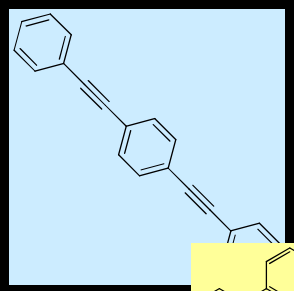

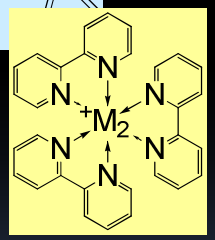

Functional Units

Step 1 Precise Arrangement of Functional Units

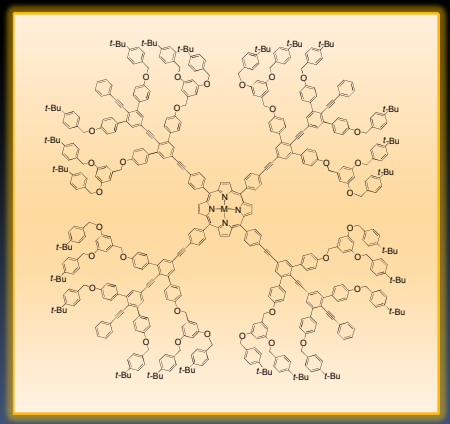

Dendrimers

Step 2 Integration of Dendrimers

Molecular Devices and Machines

Introduction of Dendrimers with Rigid Backbones

1) A dendrimer has rigid conjugated backbones within the flexible dendritic structure.

2) The rigid backbone serves as a scaffold for the construction of a well-designed assembly as well as a mediator in both the electron and energy transfer processes

3) The rigid backbones are useful for the construction of well-organized nano-scale assembly of dendrimers.

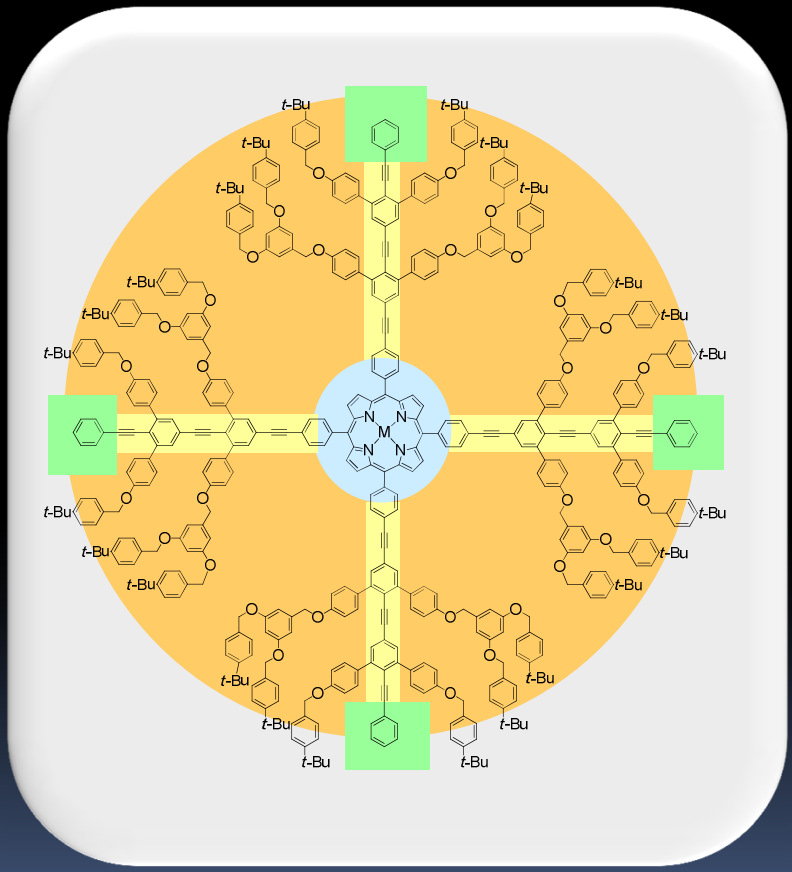

How to make the Dendrimer (Convergent Approach)

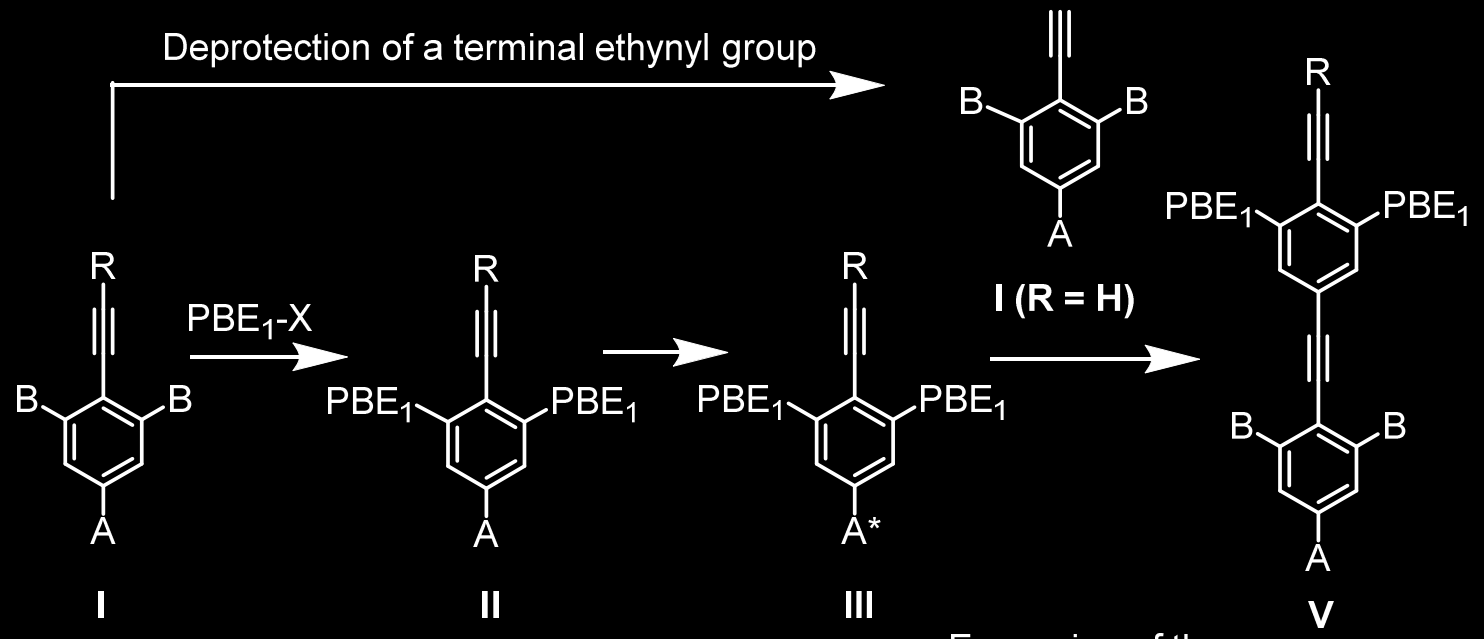

Kozaki, M.; Okada, K. *Org. Lett.* 2004, *6*, 485-488.

Synthesis of a Conjugated Chain with Branched Side Chains

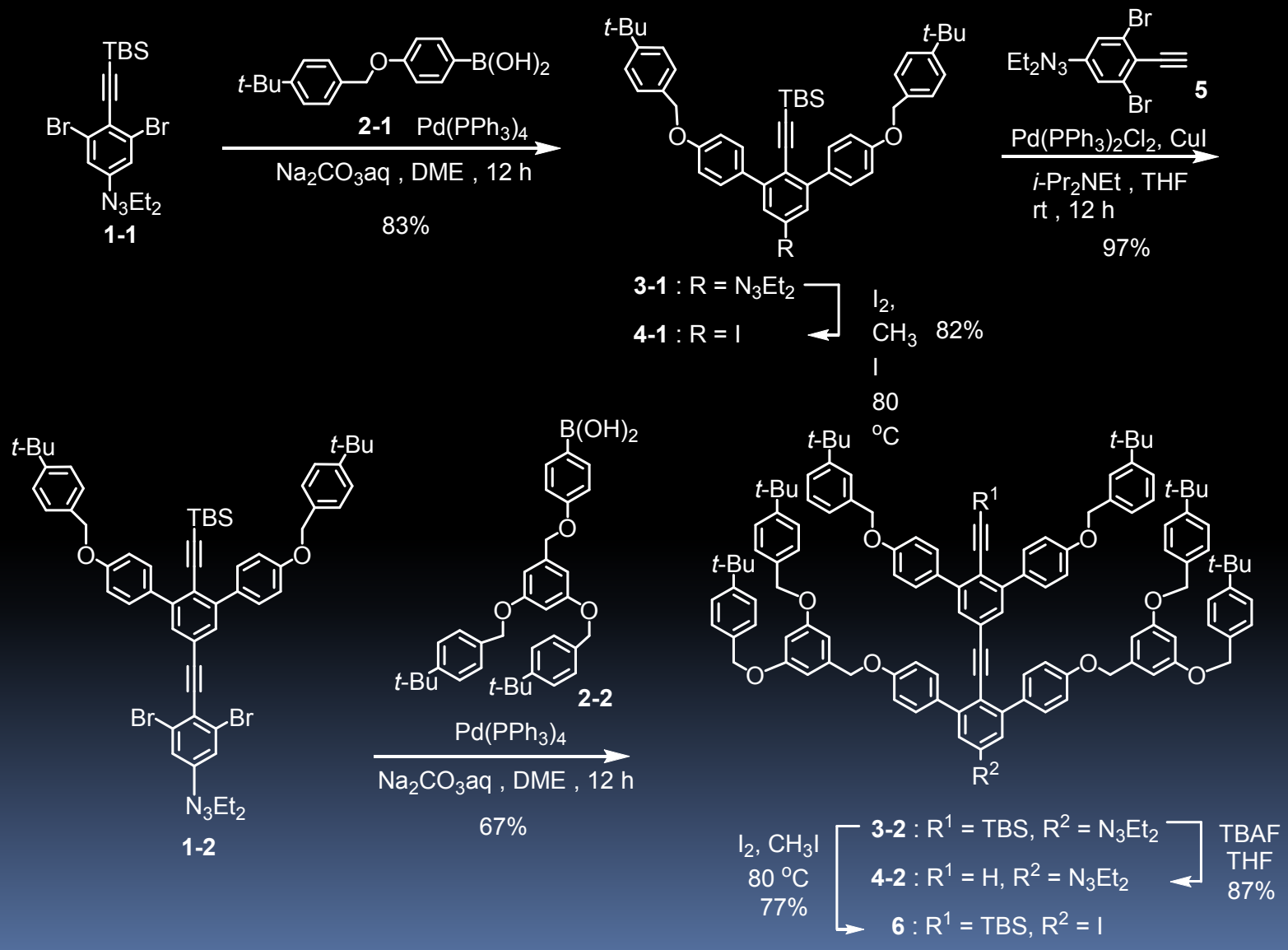

Functionalized Dendrons and Core units

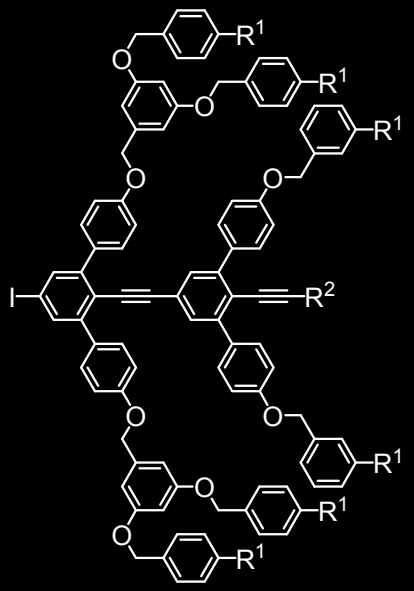

7: R^1 = H, R^2 = Ph
8: R^1 = *t*-Bu, R^2 = Ph
9: R^1 = *t*-Bu,
R^2 = 2-anthraquinonyl

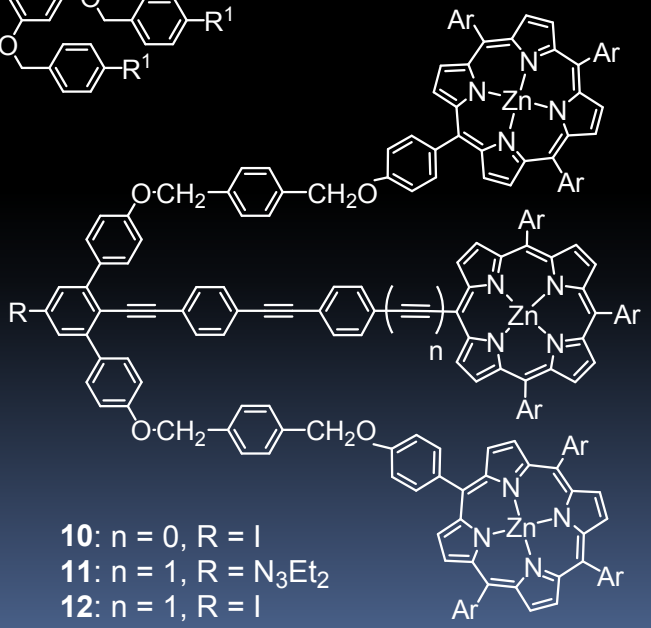

10: n = 0, R = I
11: n = 1, R = N_3Et_2
12: n = 1, R = I

Ar = 3,5-di-*tert*-butylphenyl

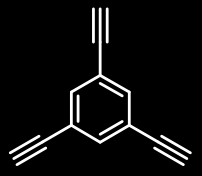

13

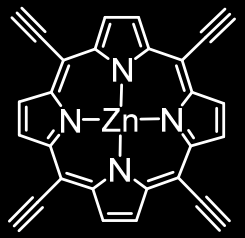

14

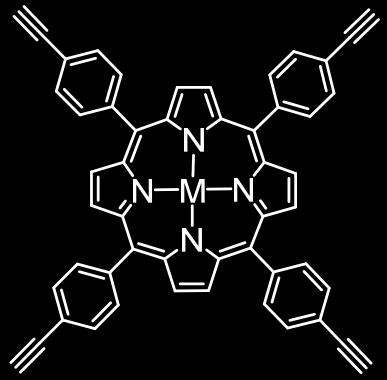

15-1: M = Zn
15-2: M = 2H

Preparation of Dendrimer with Light-Harvesting Ability

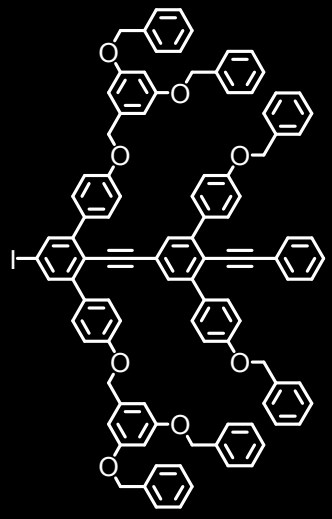

7

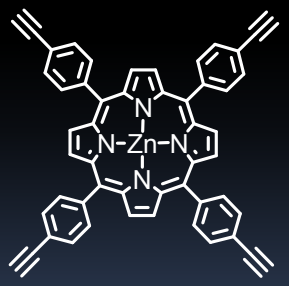

15-1

$Pd(PPh_3)_2Cl_2$, CuI

Et^iPr_2N, THF

41%

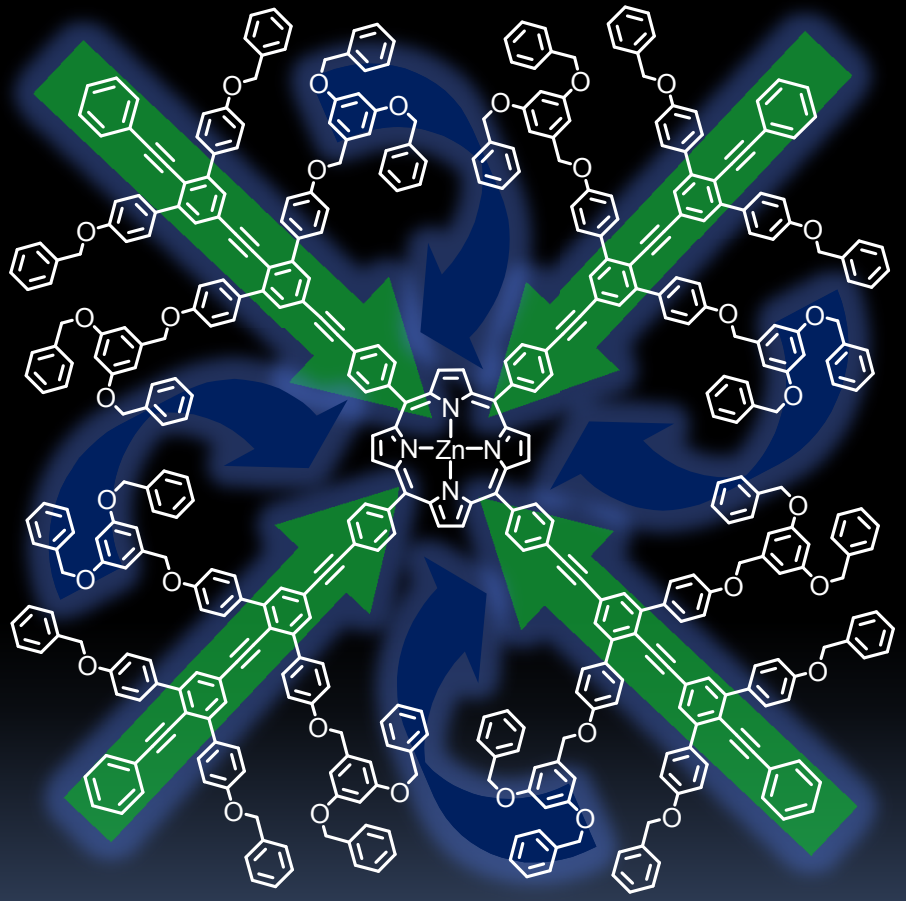

dendrimer-16 ($C_{460}H_{332}N_4O_{32}Zn$: 6486)

Advantage of the Dendrimer with Conjugated Chains

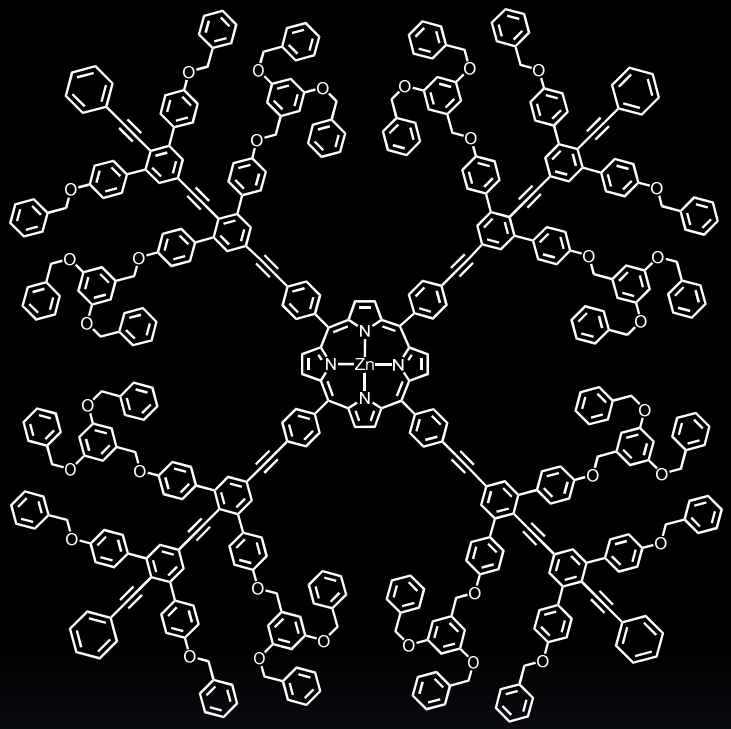

dendrimer-16

ϕ_F = 100%

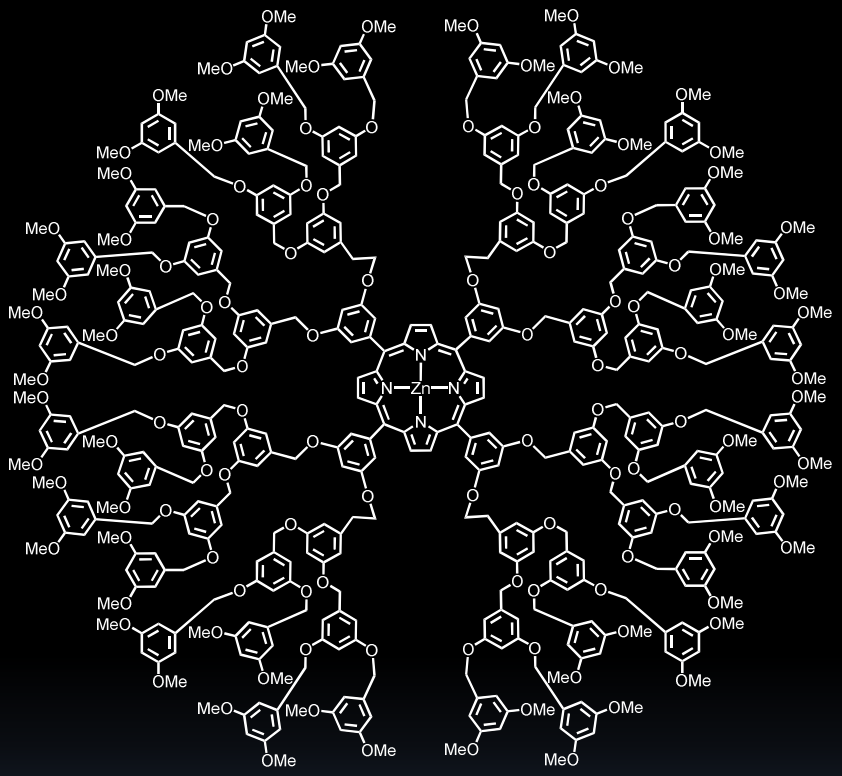

ϕ_F = 79%[1)]

(1) Jiang, D.-L.; Aida, T. *J. Am. Chem. Soc.* 1998, *120*, 10895-10901.

How to Make the Visible Light Harvester (Biomimetic Strategy)

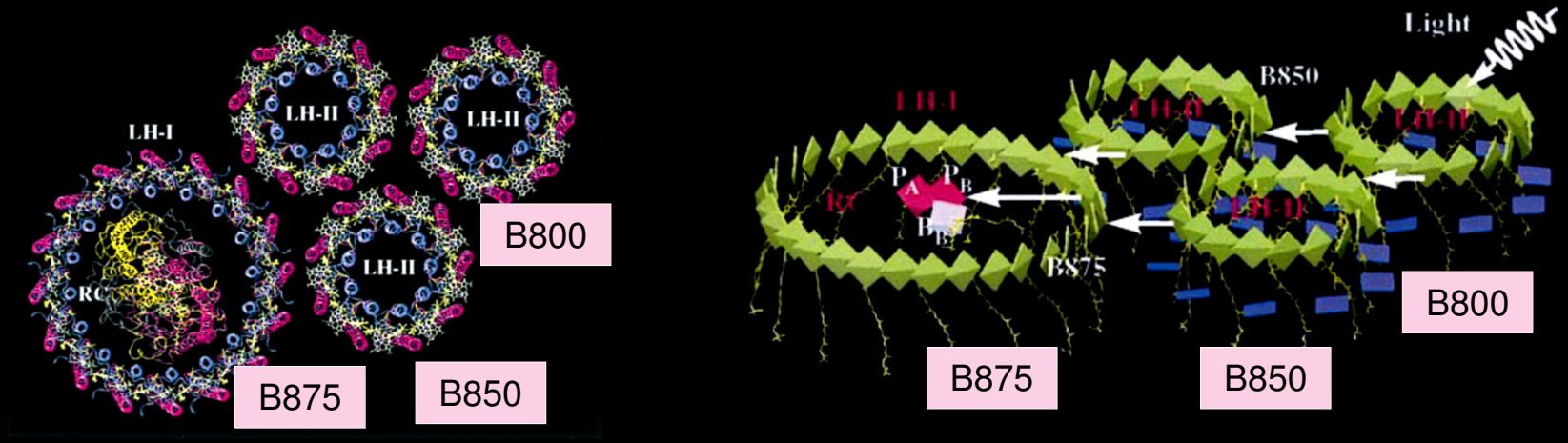

Figure 2. (a) Arrangement of pigment.protein complexes in the modeled bacterial PSU of *Rb. sphaeroides*. (b) Excitation transfer in the bacterial photosynthetic unit. LH-II contains two types of BChls, commonly referred to as B800 (dark blue) and B850 (green), which absorb at 800 nm and 850 nm, respectively. BChls in LH-I absorb at 875 nm and are labeled B875 (green). (Hu,X.; Damjanović, A.; Ritz, T.; Schulten, K. *Proc. Natl. Acad. Sci. USA* 1998, *95*, 5935-5941.)

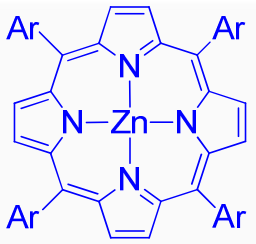

TP-Por

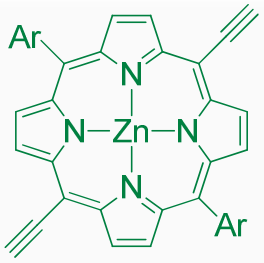

DE-Por

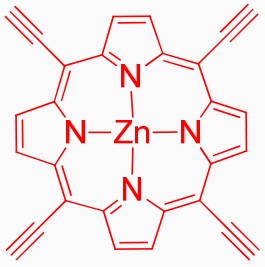

TE-Por

Strategic Arrangement of Porphyrins using the Dendritic Architecture

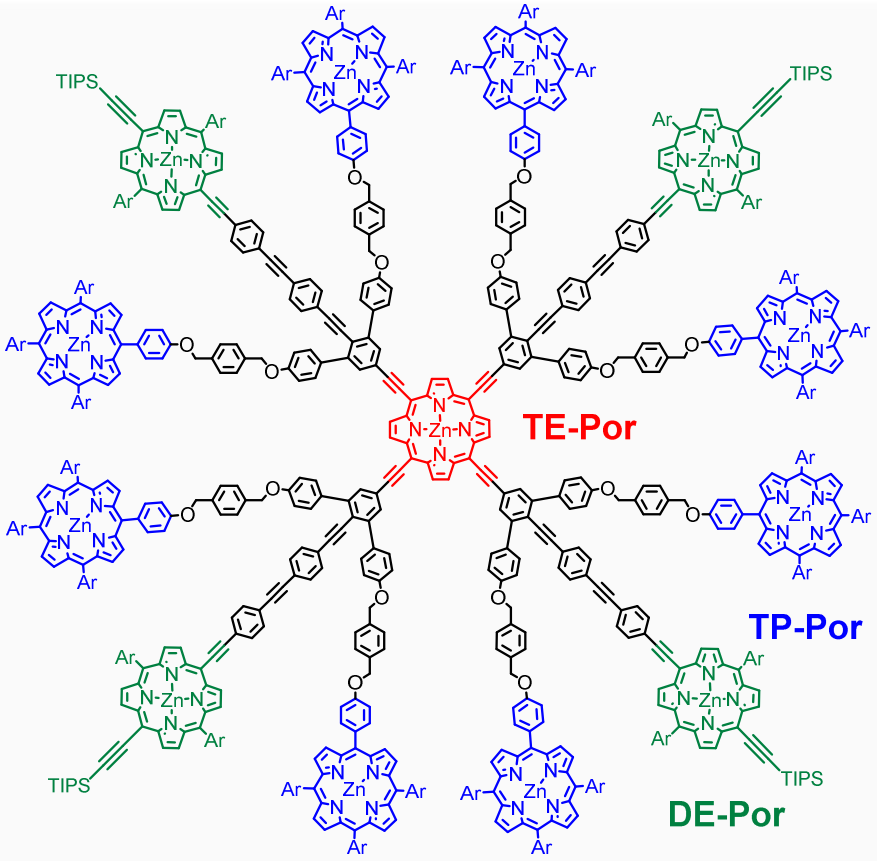

Ar = 3,5-di-*tert*-butylphenyl

dendrimer-17 ($C_{1016}H_{1028}N_{52}O_{16}Si_4Zn_{13}$: 15186)

Uetomo, A.; Kozaki, M.; Suzuki, S.; Yamanaka, K.; Ito, O.; Okada, K. *J. Am. Chem. Soc.* 2011, *133*, 13276-13279.

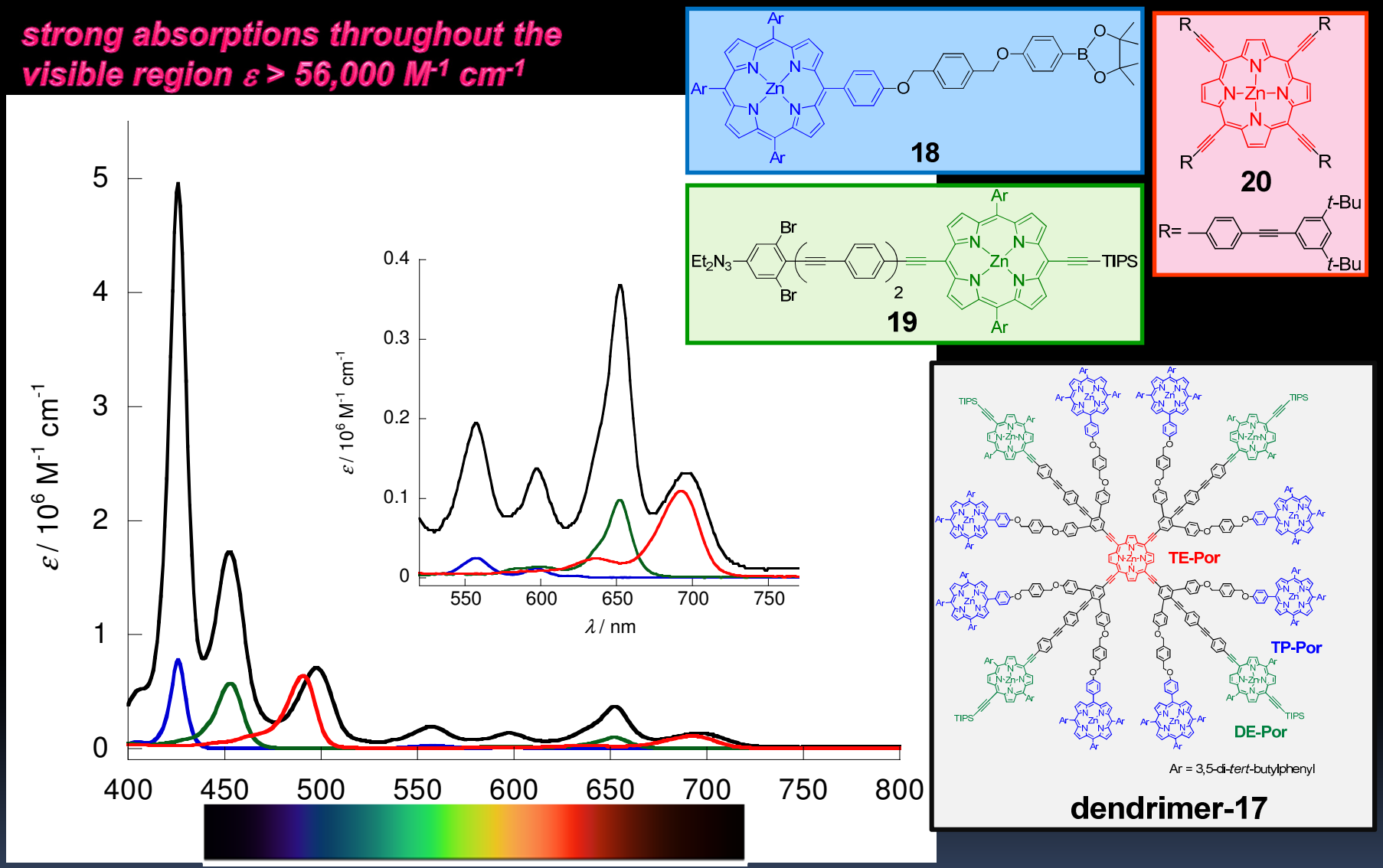

Figure 3. Absorption spectra of dendrimer-17 (black), 18 (blue), 19 (green), and 20 (red) measured in THF. The inset shows expanded absorption spectra in the Q-band region.

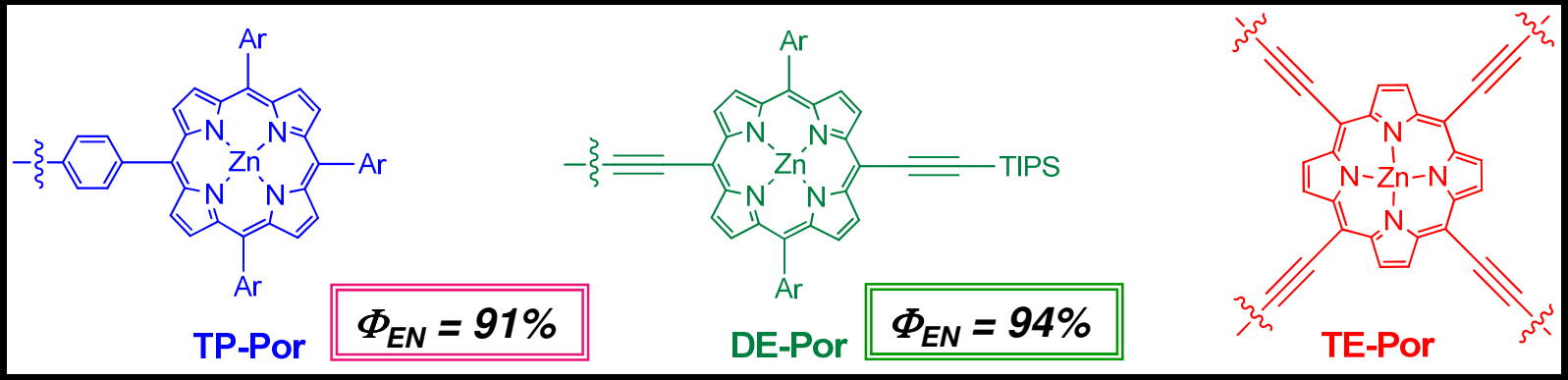

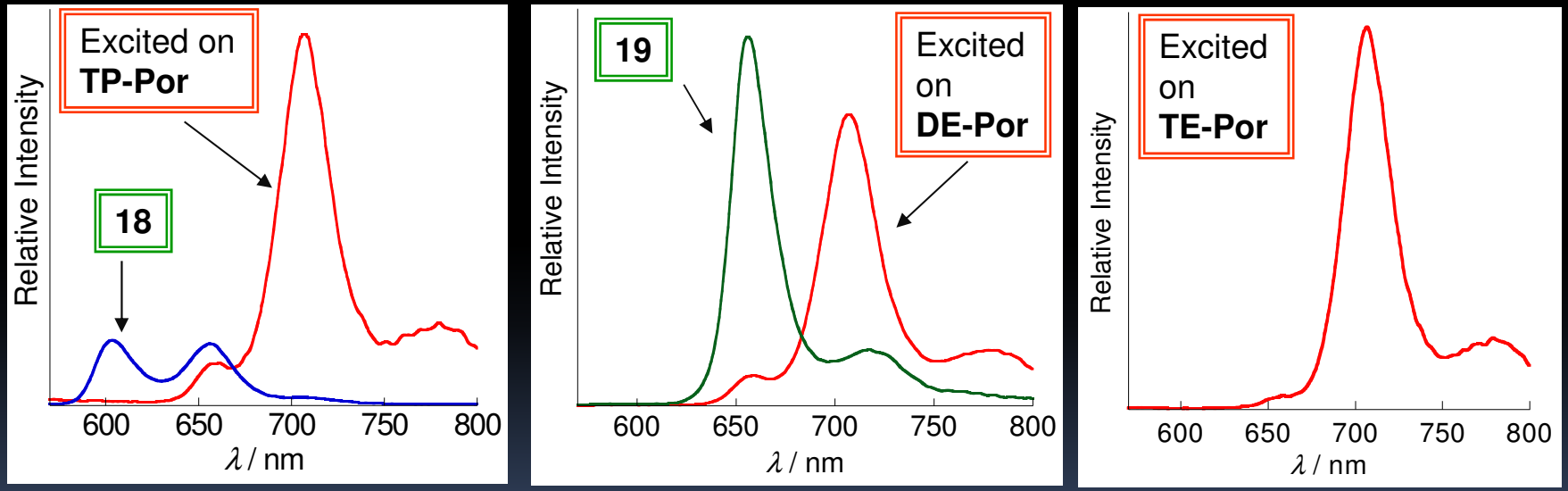

Figure 4. Steady-state fluorescence spectra of (a) dendrimer-**3** (red) and **11** (blue) (λ_{ex} = 426 nm), (b) dendrimer-**3** (red) and **12** (green) (λ_{ex} = 453 nm), and (c) dendrimer-**3** (λ_{ex} = 498 nm) measured in THF. Fluorescence intensities are measured after normalizing the absorbance at excitation wavelength.

Effective Light Harvesting Antenna

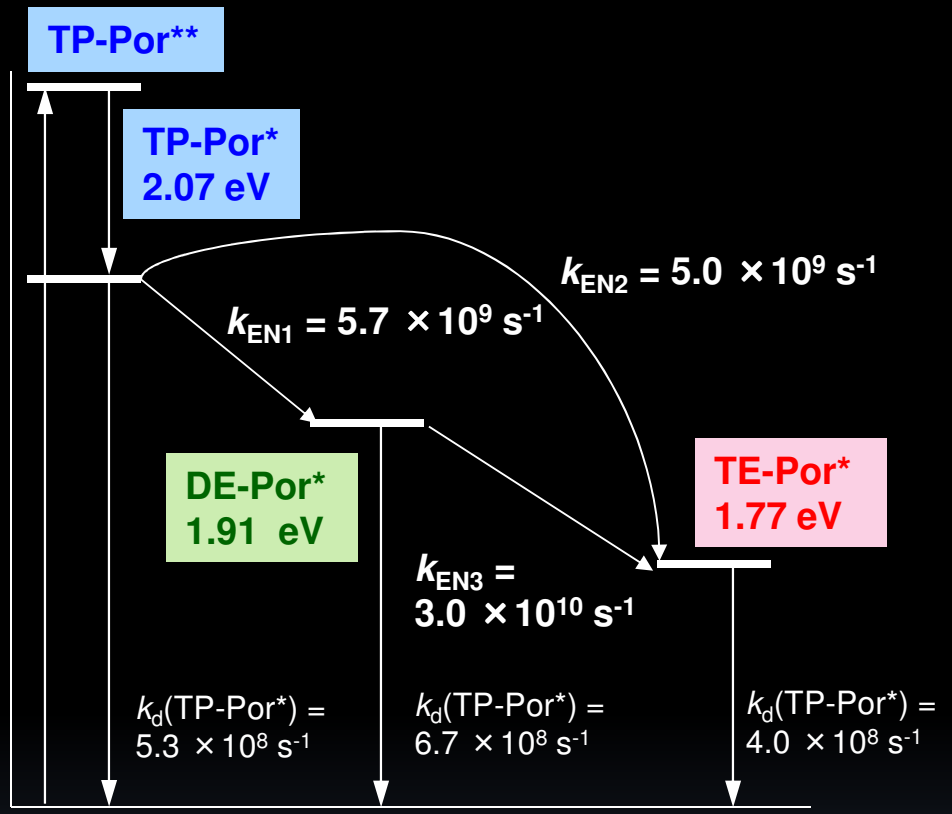

98% quantum efficiency

96% total quantum efficiency

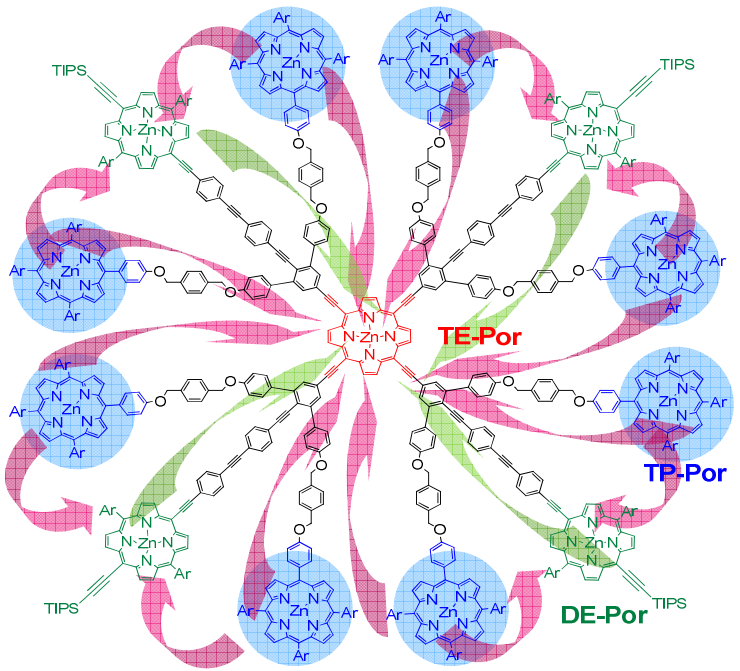

dendrimer-17

Ar = 3,5-di-*tert*-butylphenyl

Fast energy transfer through conjugated chains

Figure 9. Energy diagram and relaxation process from an excited states of **TP-Por** in dendrimer-**17**. * and ** denote the first and the second excited states, respectively.

Dendrimer with both Light-Harvesting and Charge-separating Properties

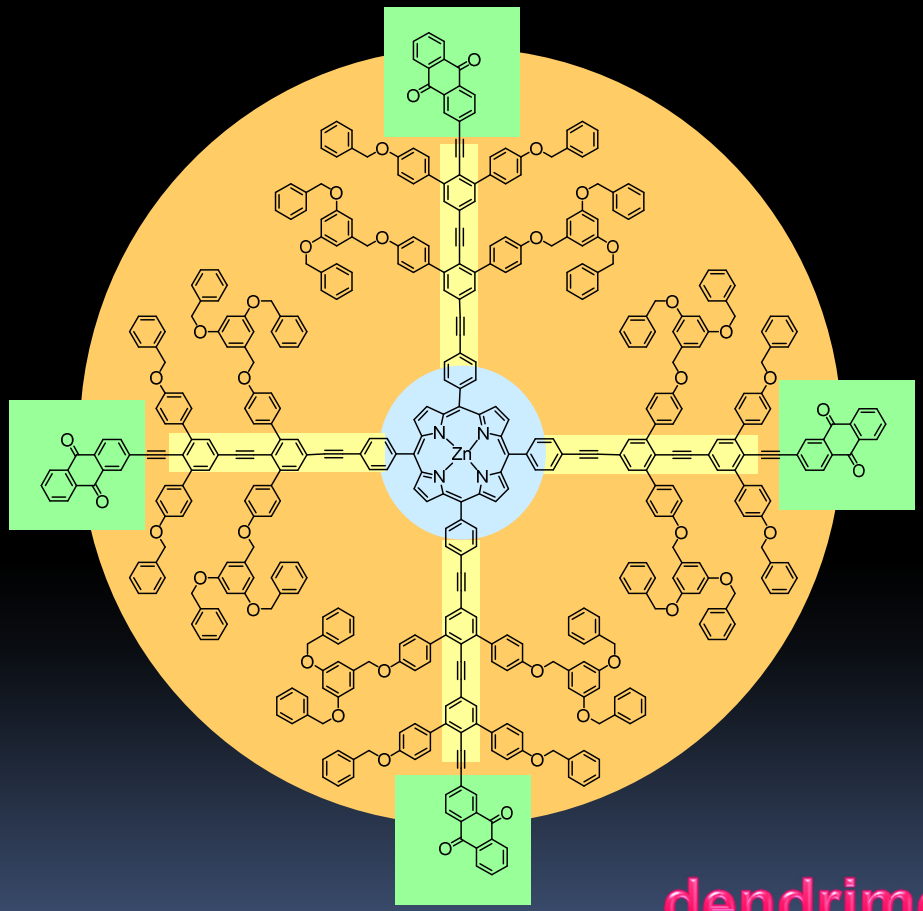

dendrimer-21

Charge-Separating Properties of the Dendrimer

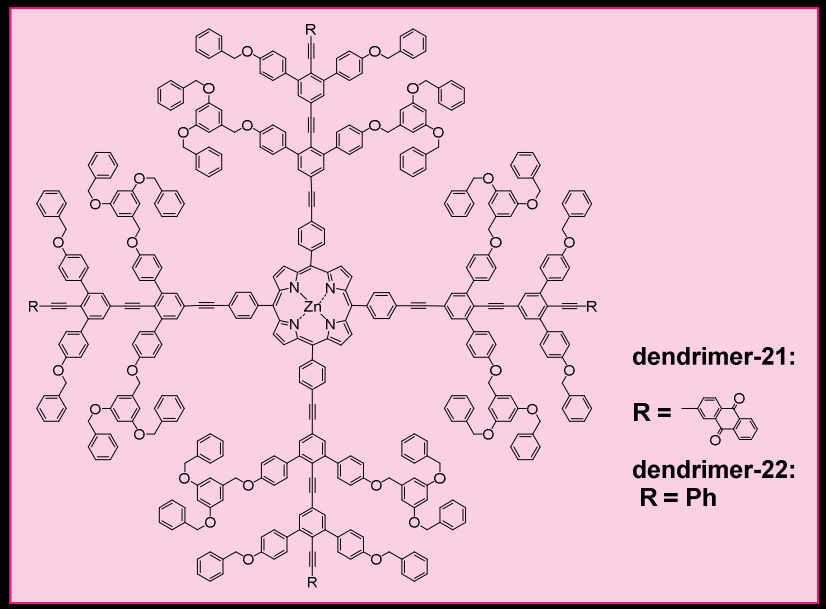

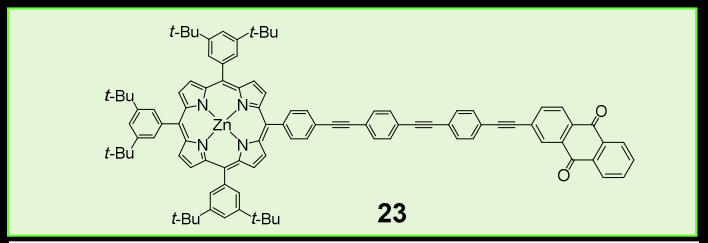

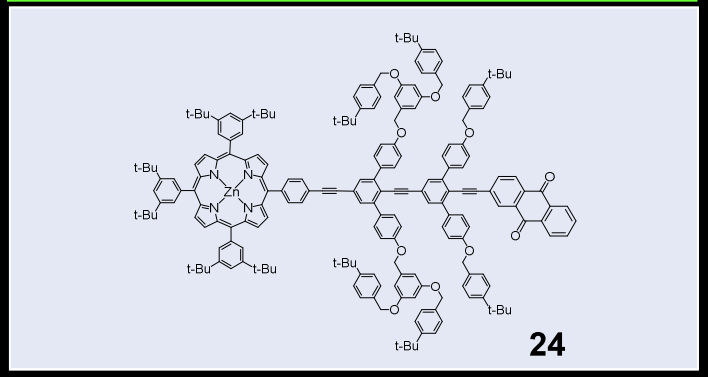

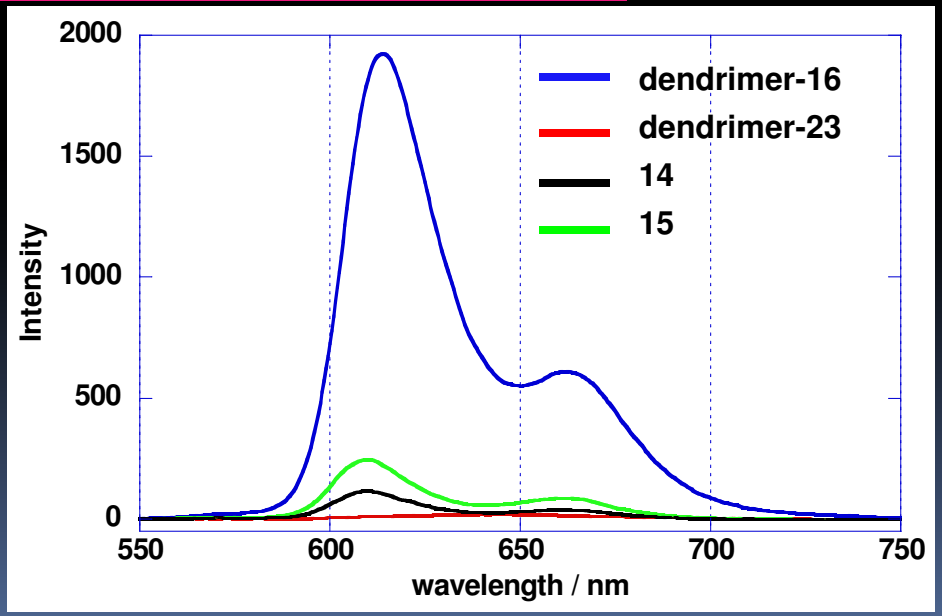

Figure 10. Fluorescence spectra of dendrimer-**1** and -**2, 14**, and **15** in DMF.

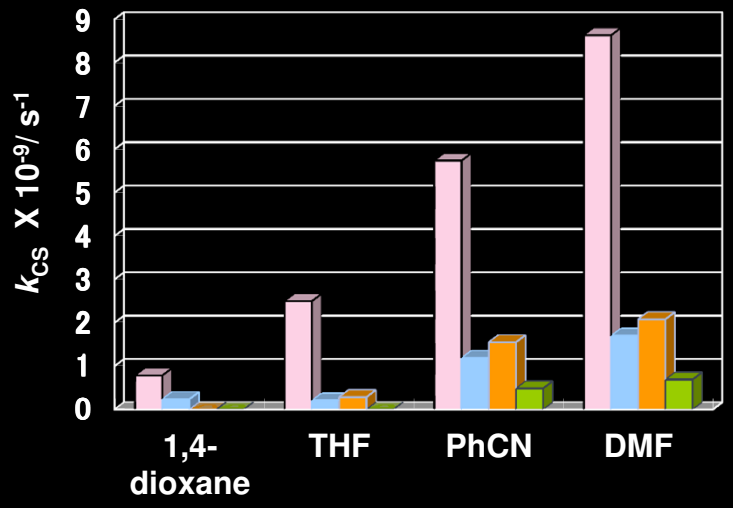

Figure 11. Charge-separation rate constants (k_{CS}) from the the excited singlet state of ZnP to AQ.

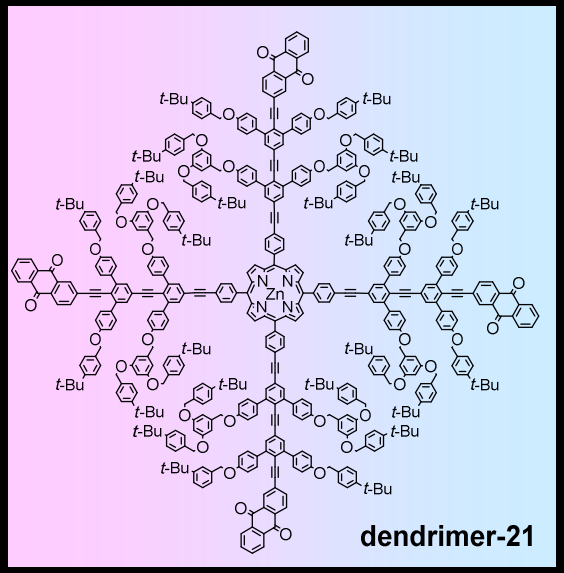

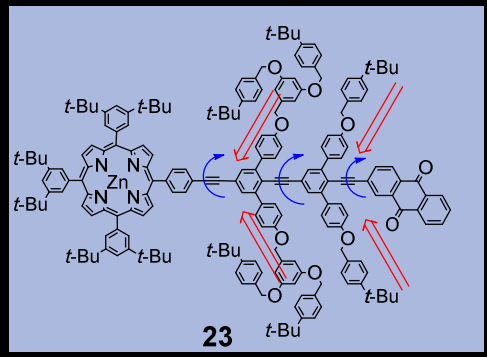

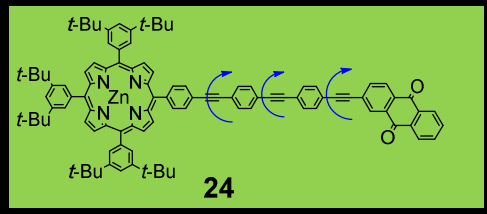

Table 2. Charge-separation rate constants (k_{CS}) from the the excited singlet state of ZnP to AQ.

Compds.	k_{CS} / s^{-1} [a]			
	1,4-dioxane	THF	benzonitrile	DMF
dendrimer-1	0.782 × 10^9 (35%)	2.50 × 10^9 (63%)	5.74 × 10^9 (88%)	8.63 × 10^9 (92%)
dendrimer-1	0.238 × 10^9 (65%)	0.208 × 10^9 (37%)	1.19 × 10^9 (12%)	1.70 × 10^9 (8%)
14	-	0.284 × 10^9	1.55 × 10^9	2.08 × 10^9
15	-	-	0.486 × 10^9	0.691 × 10^9

[a] Fluorescence lifetimes of dendrimer-**1** were used as a standard ($(t_f)_{ref}$).

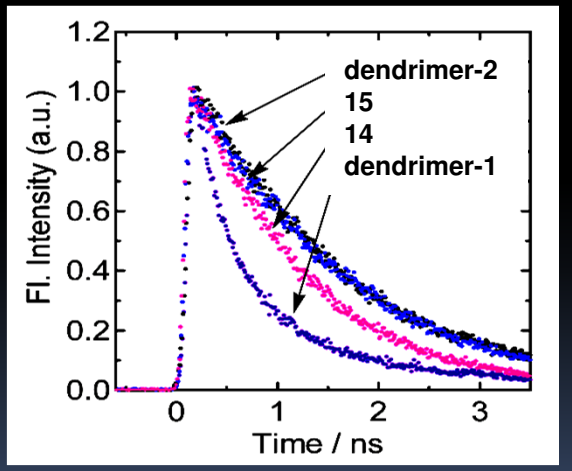

Figure 12. (a) Fluorescence decays of dendrimer-**1** and -**2, 14**, and **15** in DMF at around 610 nm-670 nm range.

Kozaki, M.; Akita, K.; Okada, K. *Org. Lett.* **2007**, *9*, 1509-1512. Kozaki, M.; Akita, K.; Okada, K.; Islam, D.-M. S.; Ito, O. *Bull. Chem. Soc. Jpn.* **2010**, *83(10)*, 1223-1237.

Dendrimers with Conjugated Backbones

Charge-separating System

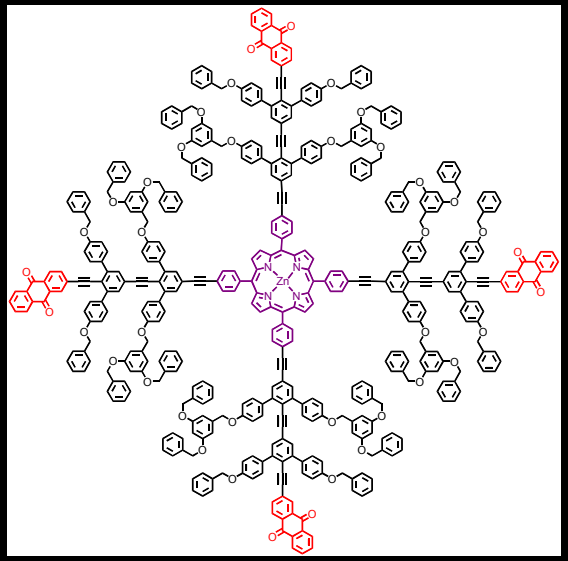

Org. Lett. 2007, *9*, 1509-1512.
Bul. Chem. Soc. Jpn. 2010, *83*, 1223-1237.

Light-harvesting Antenna

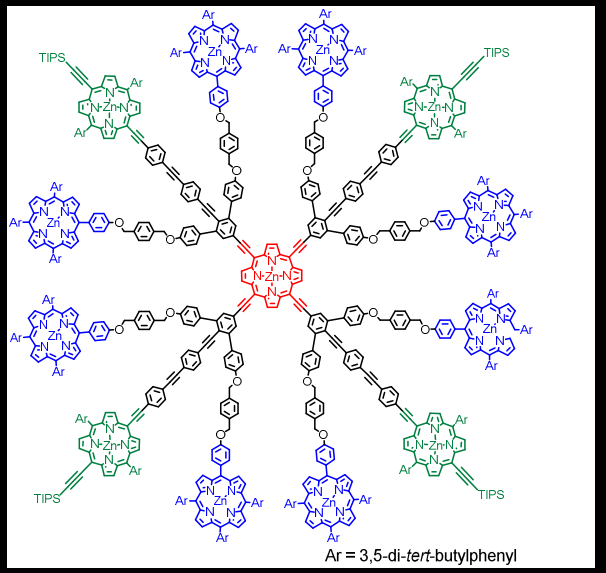

J. Am. Chem. Soc. 2011, *133*, 13276-13279.

Establishment of the Synthetic Methodology for the Construction of a Nanoscale Array of Denderimers

Precise arrangement of Dendrimers Creation of advanced functions that are not realized with low molecular weight materials

Methodology for the Construction of Nanoscale Architectures

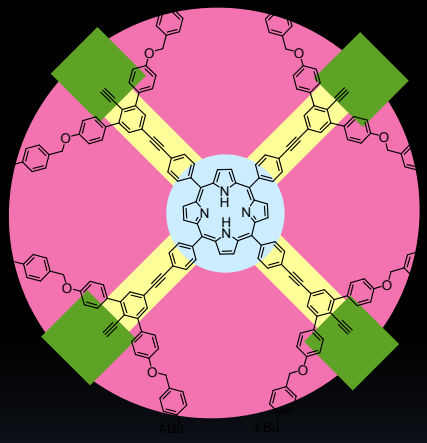

A_4-type Dendrimer

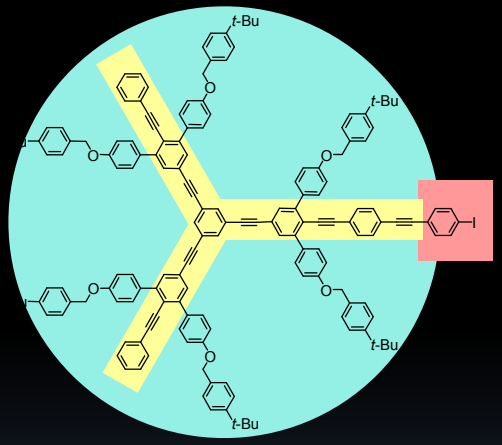

AB_2-type Dendrimer

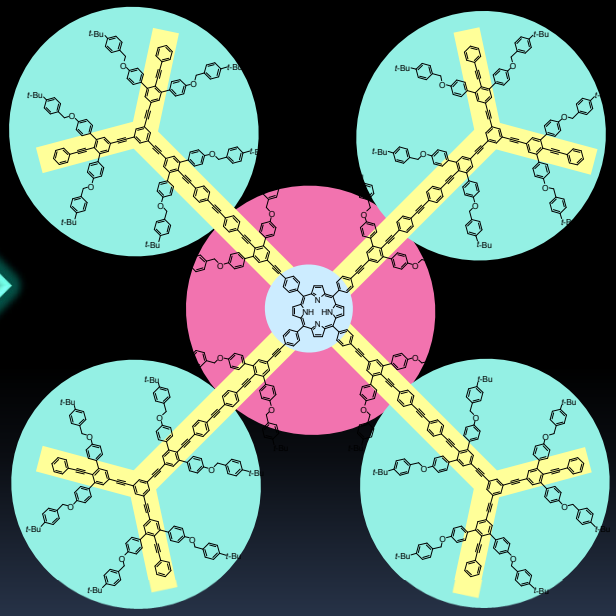

Advantages of the Assembling Method

- The well-defined arrangement of connecting sites and rigidity of conjugated backbones ensure the accurate formation of pre-designed architectures.
- A well-designed and highly organized array of functional units can be prepared using the conjugated backbones as a scaffold. Moreover the interaction among these units is adjustable by structural modification of backbones.

Dendrimers with Necked and Buried Couplers

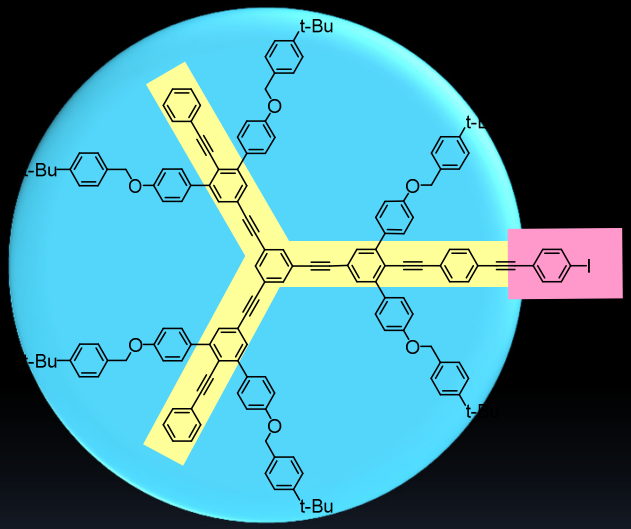

AB_2-type Dendrimer with Necked Coupler

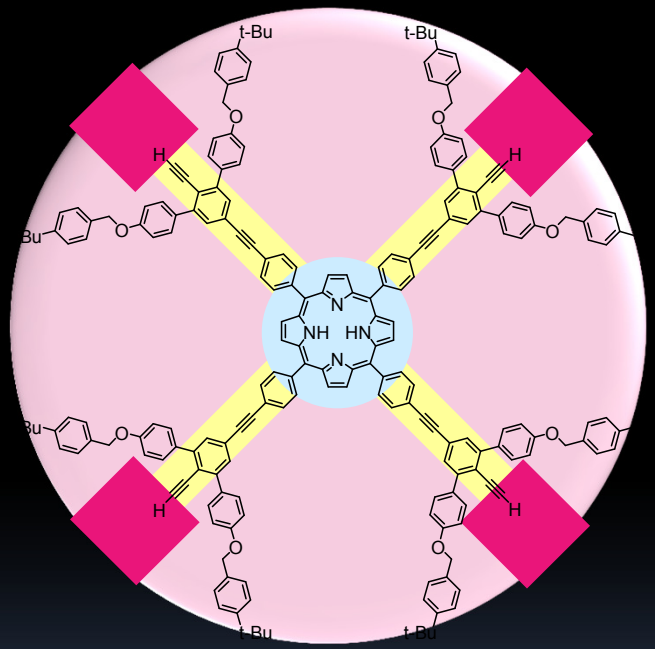

A_4-type Dendrimer with Buried Coupler

Integration of Dendrimers

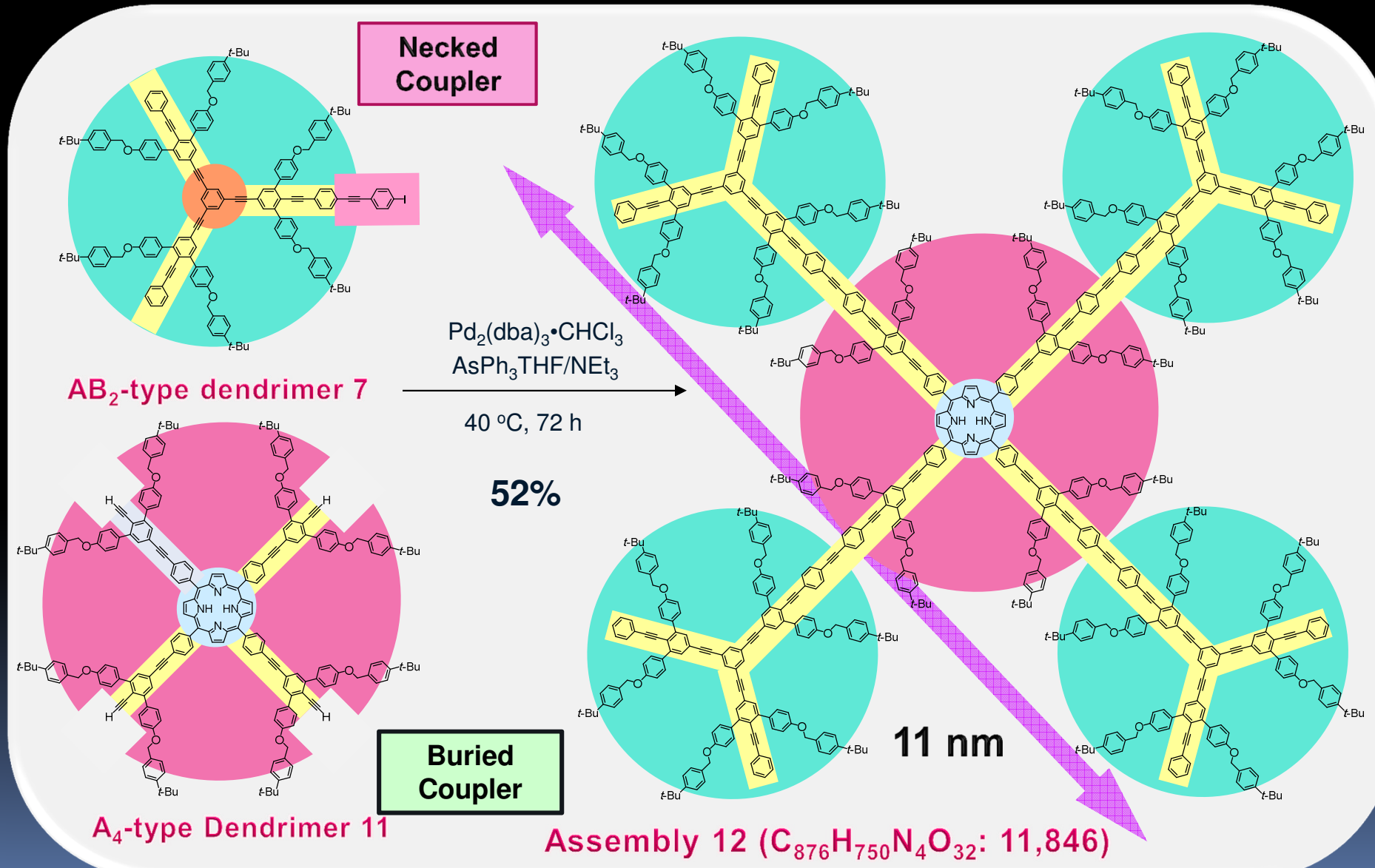

Synthesis of Porphyrin Dendrimers

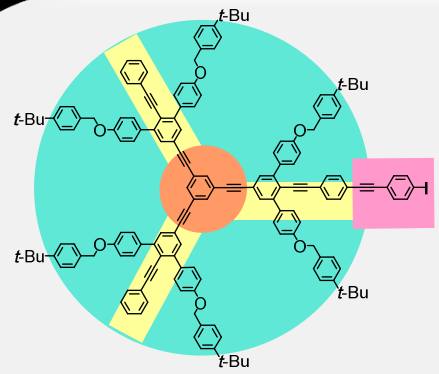

AB_2-type Dendrimer 7

$Pd_2(dba)_3 \cdot CHCl_3$, $AsPh_3$

$THF\text{-}NEt_3 = 5{:}1$

45 °C, 3 days

17%

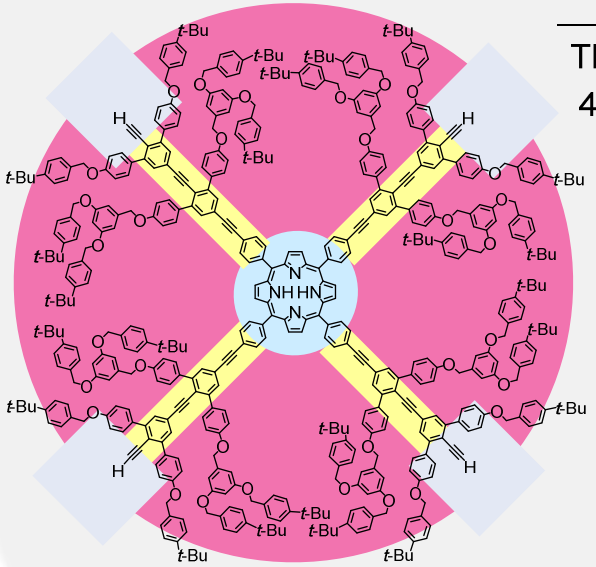

A_4-type Dendrimer 15

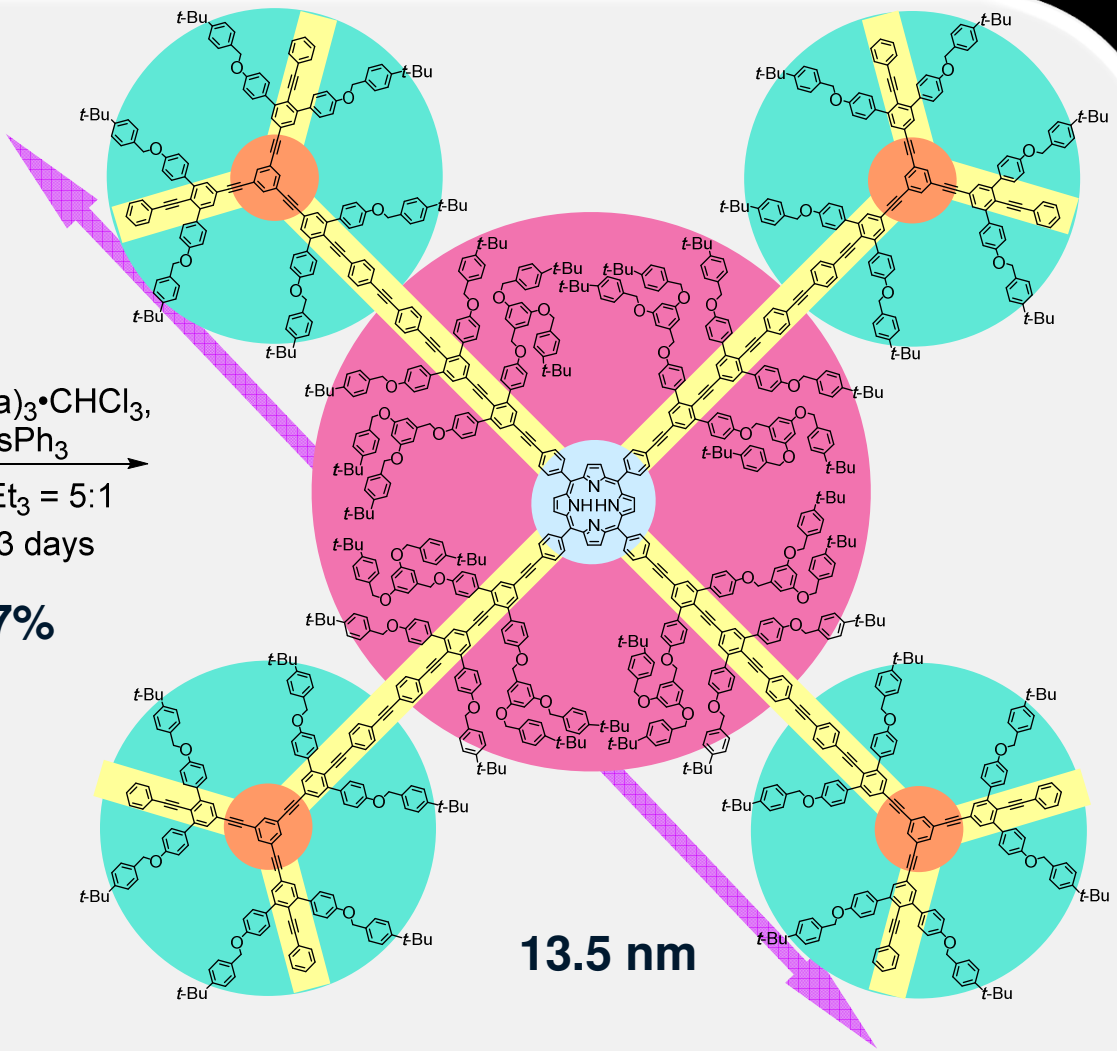

13.5 nm

Assembly 16 ($C_{1188}H_{1070}N_4O_{56}$: 16,299)

Iterative Convergent / Divergent Strategy

Click Reaction (CuAAC reaction)

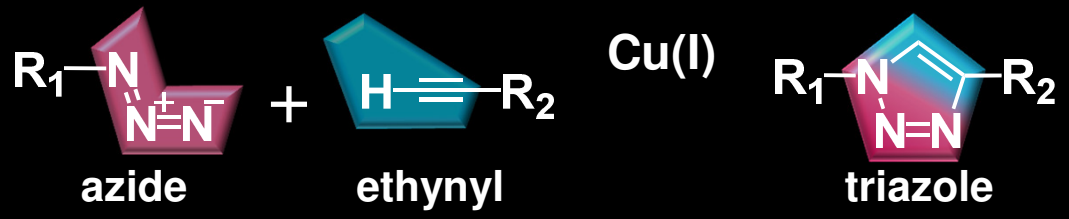

Simple procedure and clean conversion

Iterative Convergent / Divergent Strategy

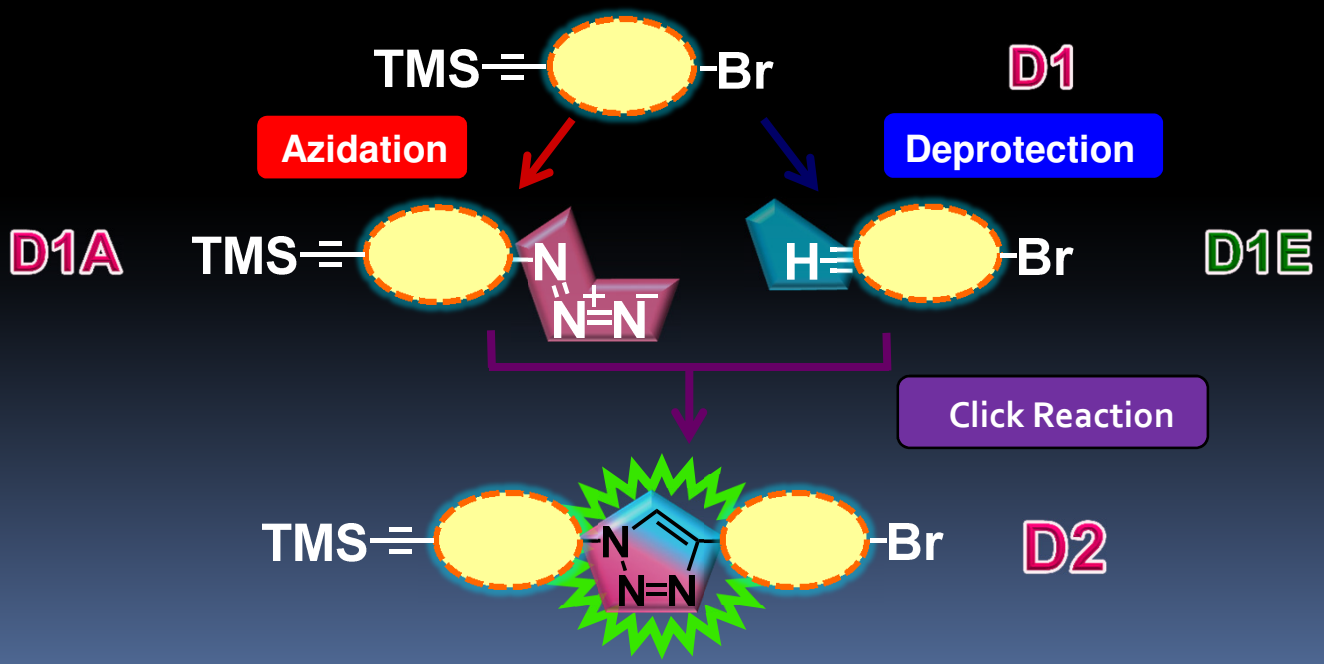

Iterative Convergent / Divergent Synthesis

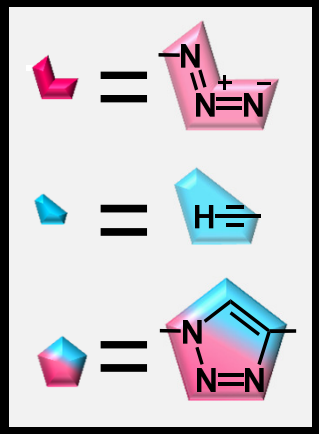

Click Reaction
(CuI, *i*-Pr_2NEt / THF)

Deprotection
(K_2CO_3, 18-crown-6
MeOH / CH_2Cl_2)

Azidation
(NaN_3, DMF)

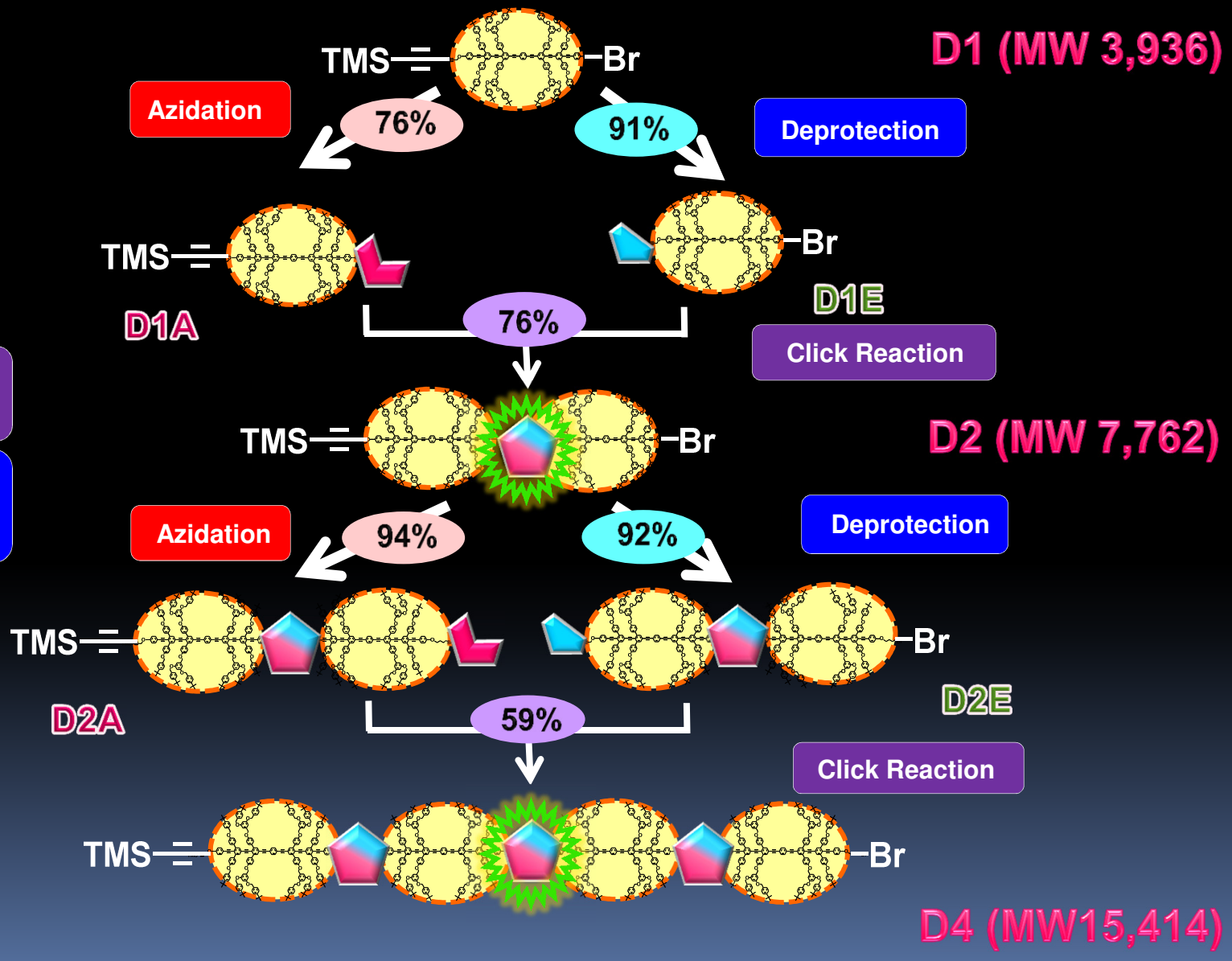

Iterative Convergent / Divergent Synthesis

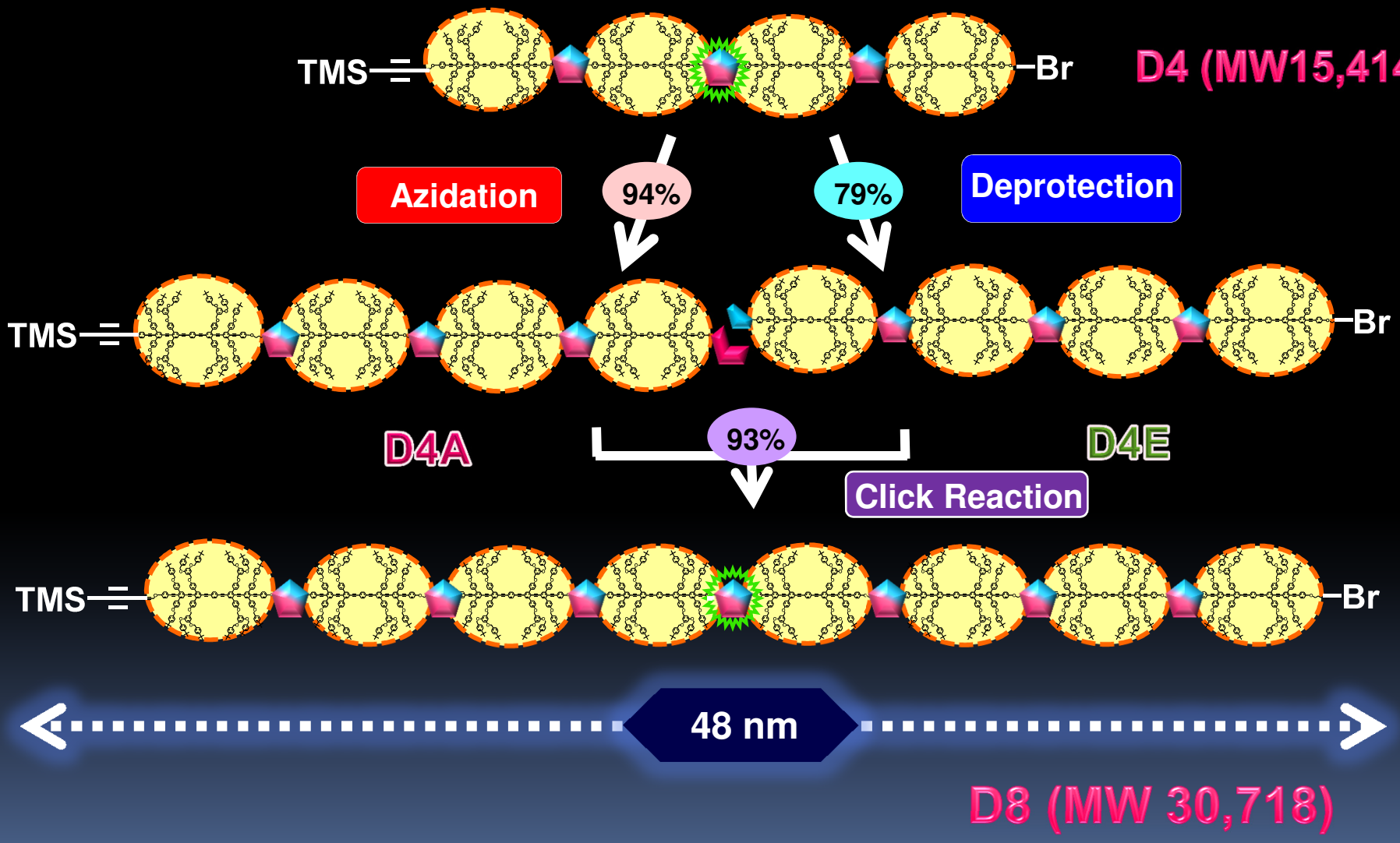

Conclusion

Dendrimers containing rigid conjugated backbones were prepared by a convergent method where the attachment of dendritic branches and the extension of phenylene-ethynylene units were alternatively manipulated on the structure of AB_2 substituted diphenylacetylene in a combination with Suzuki-Miyaura and Sonogashira cross-coupling reactions.

These dendrimer structures were applied for the construction of several light-harvesting antennas and charge-separating systems. The conjugated network inside the dendritic structure was shown to play an important role as a mediator in both the photoinduced energy- and electron-transfer processes.

We present a novel methodology for the stepwise construction of shape-persistent assemblies using the dendrimers with conjugated backbones as the key modular building blocks. These examples demonstrate advantage of the dendrimer with conjugated backbones for the construction of nanoscale molecular devices such as artificial photosynthetic systems.

Acknowledgment

This work was partially supported by Grants (No.23350022 and 22350066) from JSPS. We thank for Otsuka Electronics for measurements of fluorescence quantum yields.

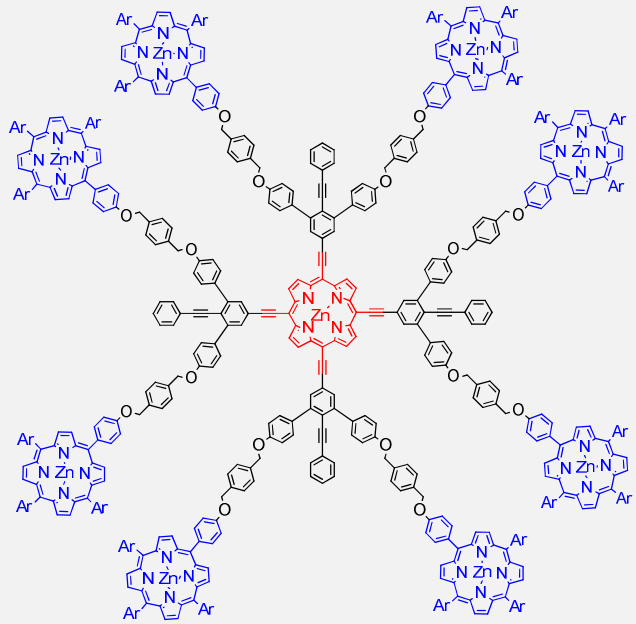

21

Ar: 3,5-di-*tert*-butylphenyl

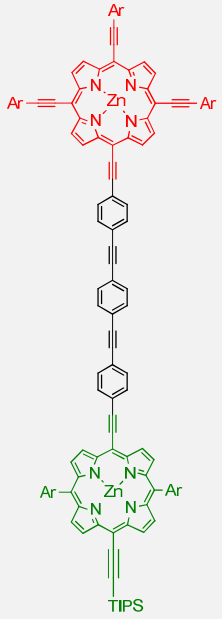

22

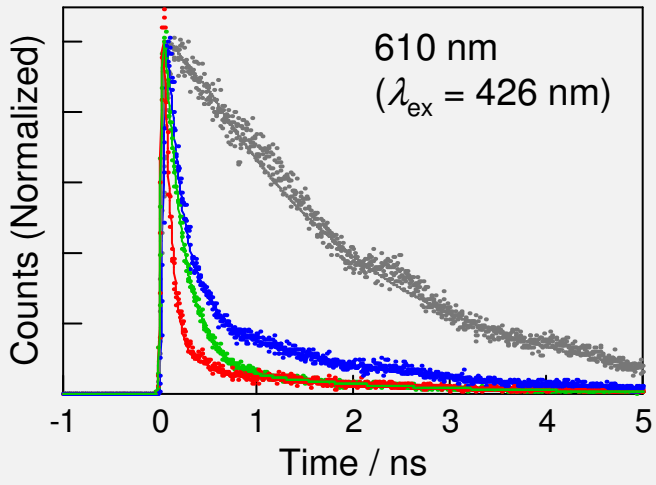

Figure 5. Fluorescence decays of **6** (red), **4** (gray), **9** (blue), and **13** (green) at 610 with λ_{ex} = 426 nm in THF.

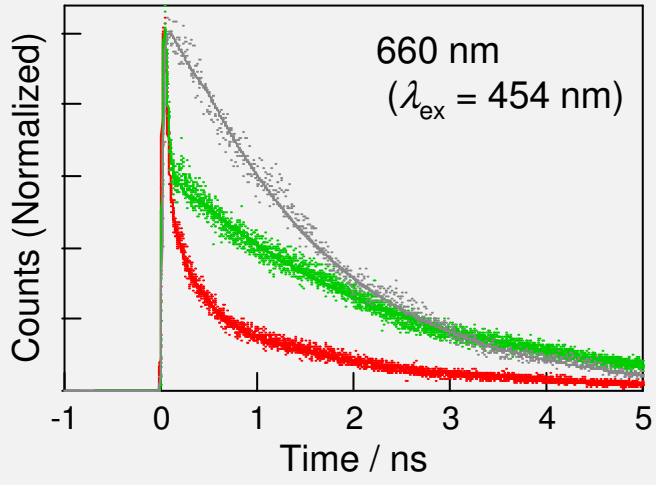

Figure 6. Fluorescence decays of **6** (red), **7** (gray), and **14** (green) at 660 with λ_{ex} = 454 nm in THF.

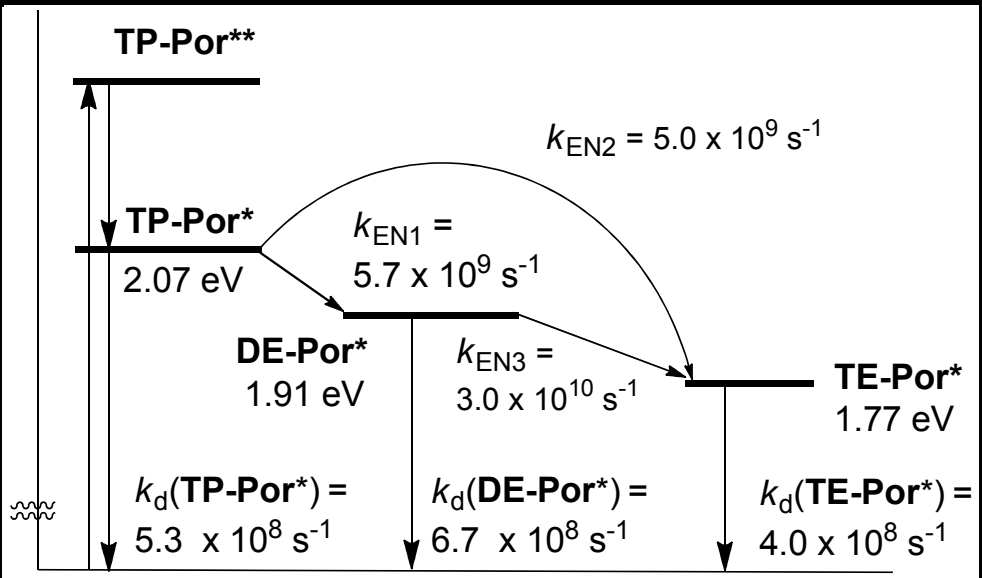

Figure 7. Energy diagram and relaxation process from an excited states of **TP-Por** in the antenna **1**. * and ** denote the first and the second excited states, respectively

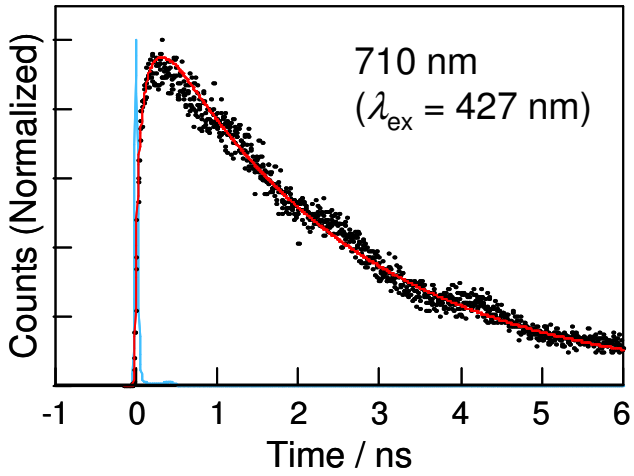

Figure 8. Fluorescence decay curve at 710 nm of **6** excited at 427 nm in THF (dots). The red solid line was obtained by the simulation. The shape decay (blue) is lamp profile.

Table 1. Photophysical data of **1, 4, 8,** and **9** in THF.

compd	λ_{ex}/nm	λ_{detect}/nm	k_{EN}/s^{-1}	energy-transfer step	calcd k_{EN} / s^{-1} [a]
6	427	610	1.2×10^{10}	**EN1**+**EN2**	-
9	427	610	5.7×10^{9}	**EN1**	2.57×10^{10}
13	427	610	5.0×10^{9}	**EN2**	1.81×10^{9}
6	456	660	3.0×10^{10}	**EN3**	9.89×10^{9}
14	456	660	3.0×10^{10}	**EN3**	9.89×10^{9}

[a] Energy transfer rates were evaluated using the Förster equation.

Light Harvesting Properties of the Dendrimer

Highly efficient (~100%) intramolecular singlet energy transfer

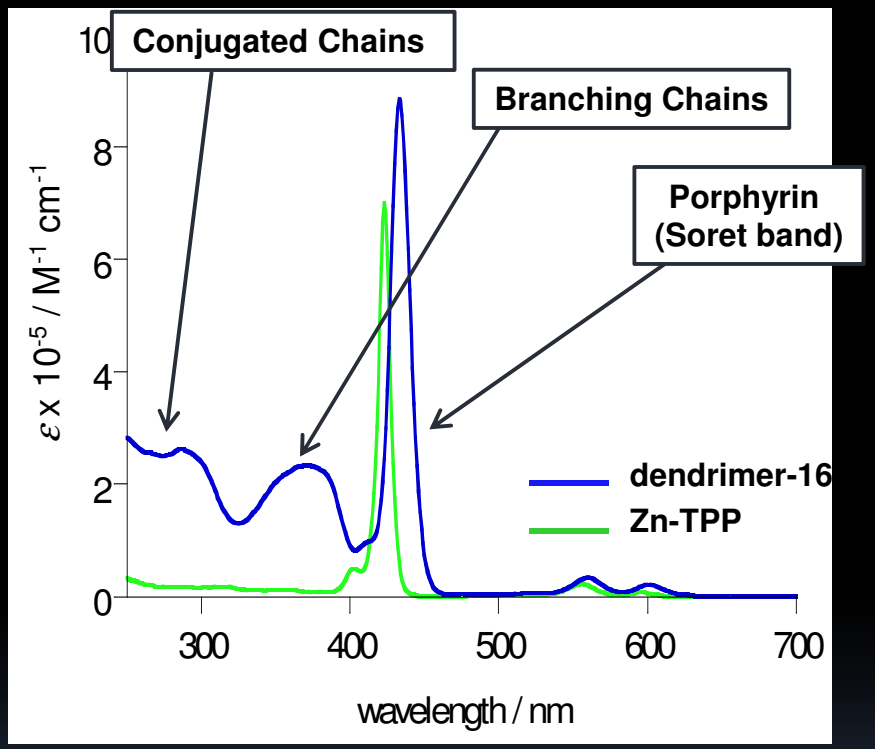

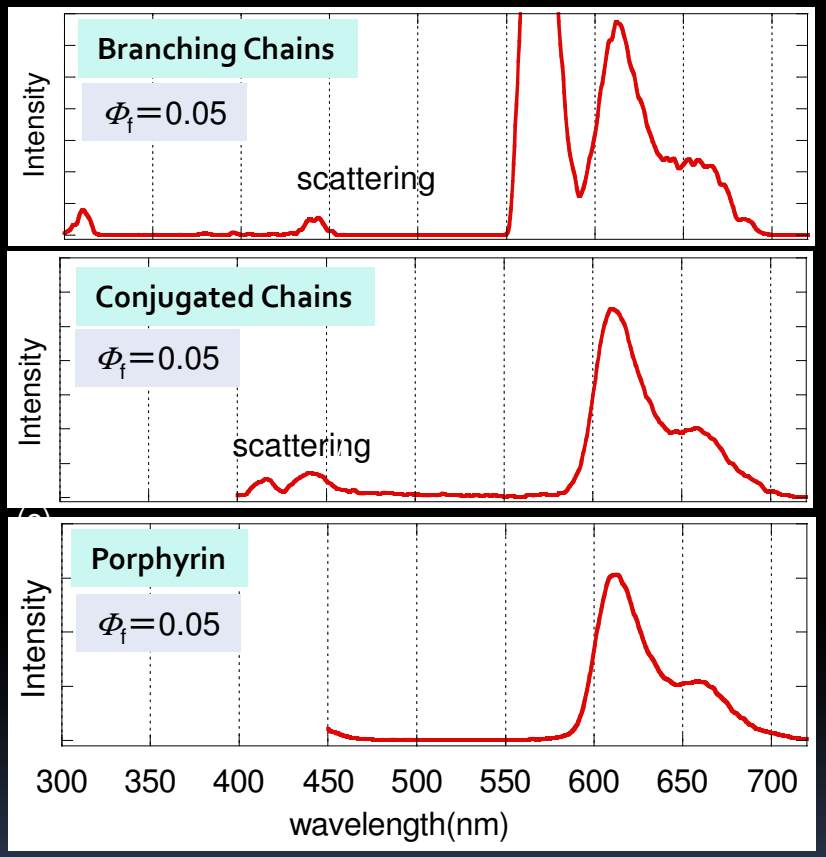

Figure 1. UV-vis spectra of dendrimer-16 and Zn-TPP in THF. (upper right) Steady-state fluorescence spectra of dendrimer-16 in THF. (lower right) (a) 286 nm excitation (The intense peak at 572 nm is the scattering of excitation light). (b) 372 nm excitation (The weak peak at 415 nm is the scattering of excitation light). (c) 433 nm excitation.

Kozaki, M.; Akita, K.; Okada, K. *Org. Lett.* 2007, *9*, 1509-1512.

Major and Minor Products

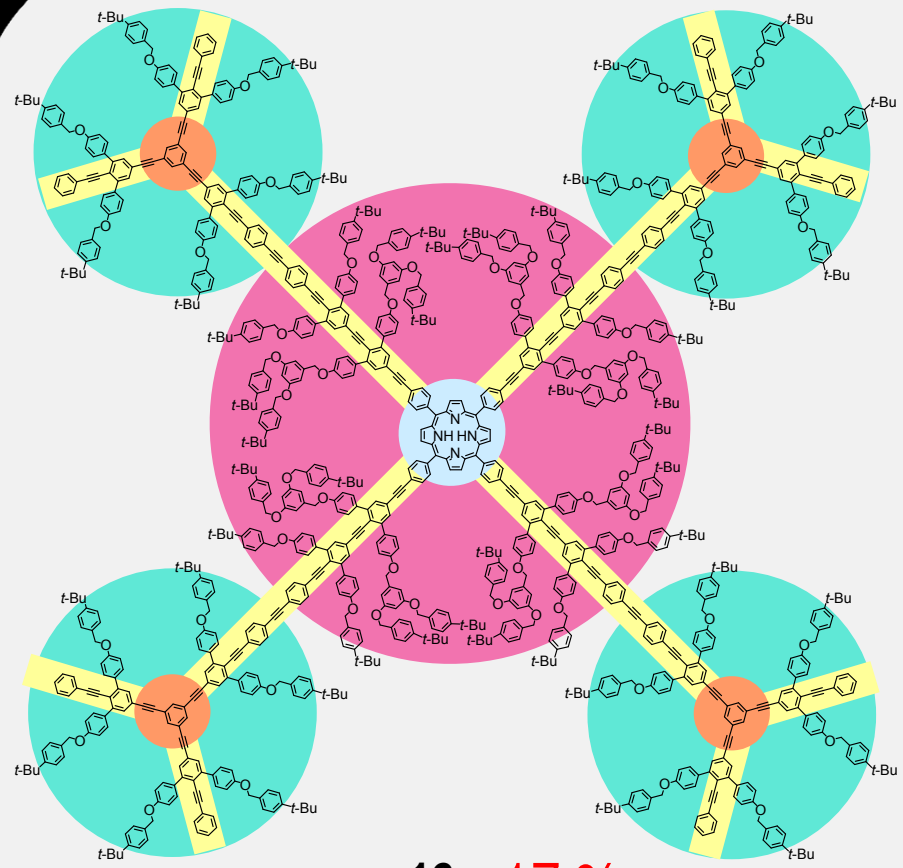

16 17 %

$C_{1188}H_{1070}N_4O_{56}$ MW 16,299

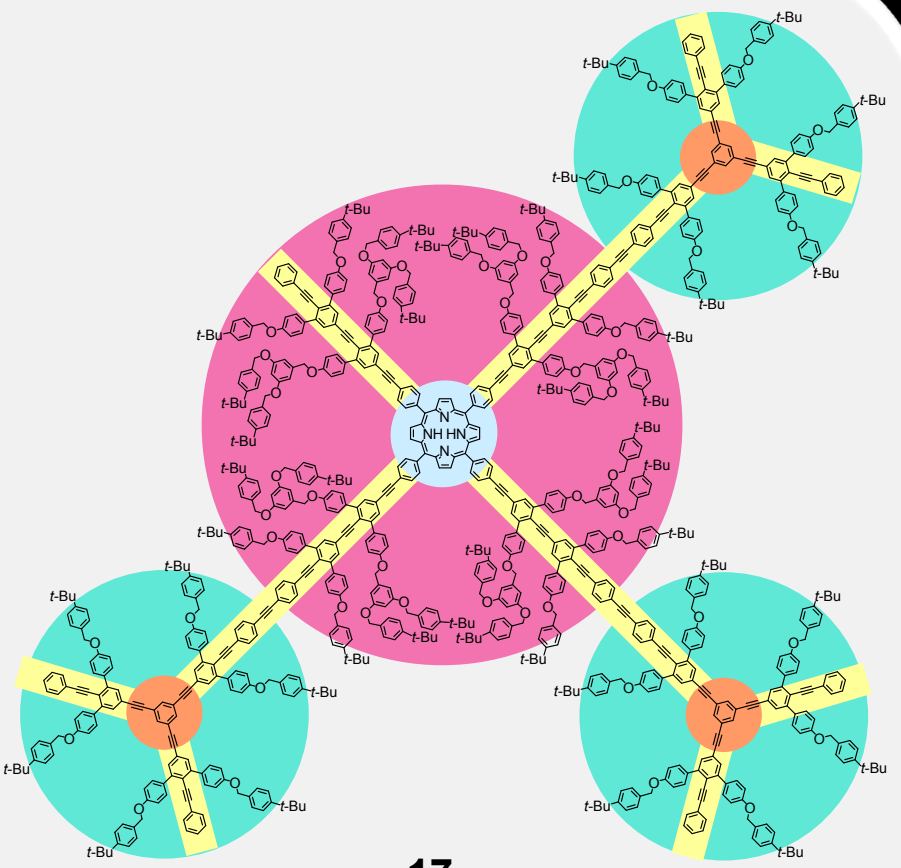

17 32 %

$C_{1030}H_{934}N_4O_{50}$MW 14,172

Synthesis of Dendrimers

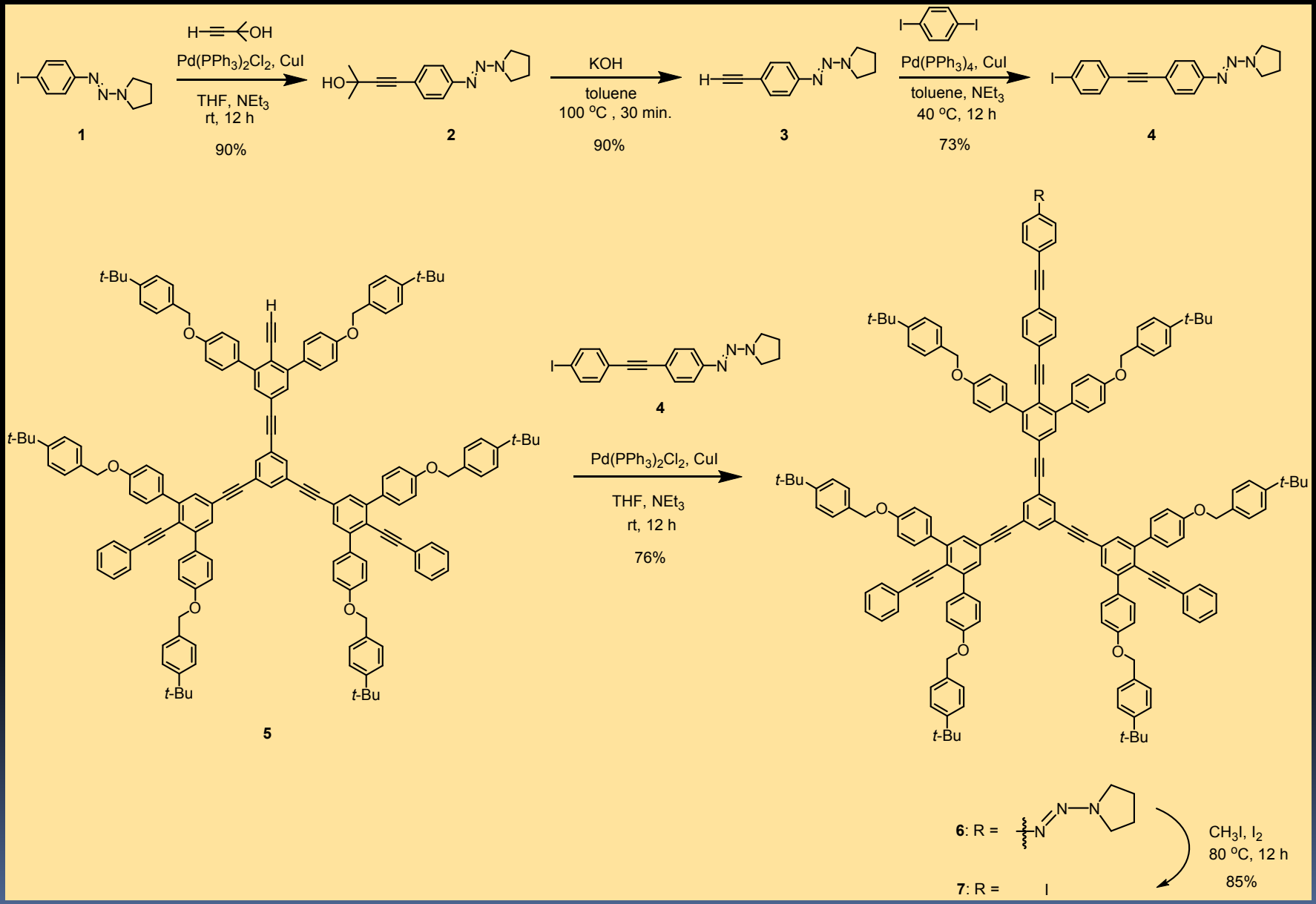

Synthesis of Porphyrin Dendrimers

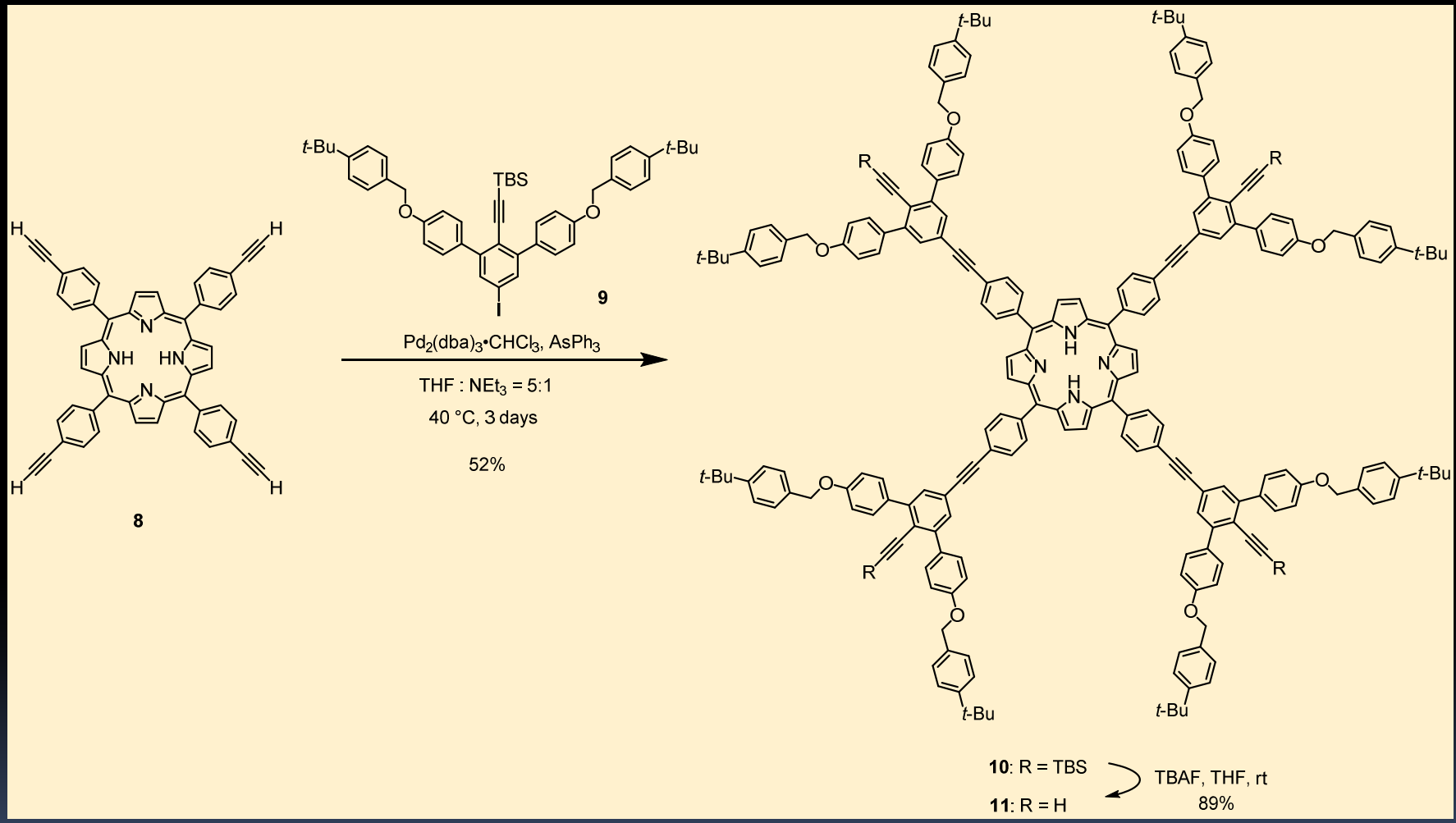

Synthesis of Porphyrin Dendrimers

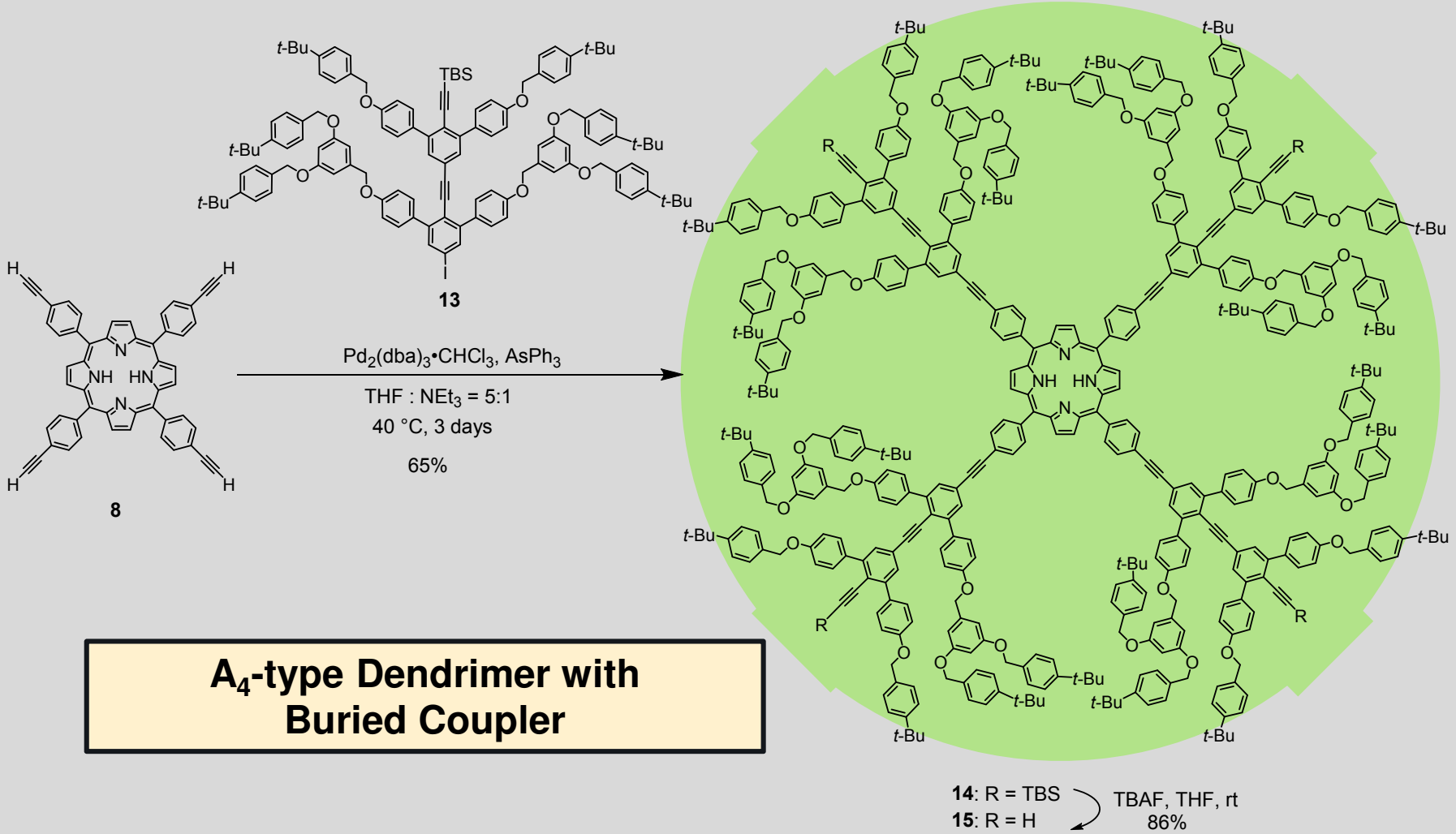

A_4-type Dendrimer with Buried Coupler

Summary

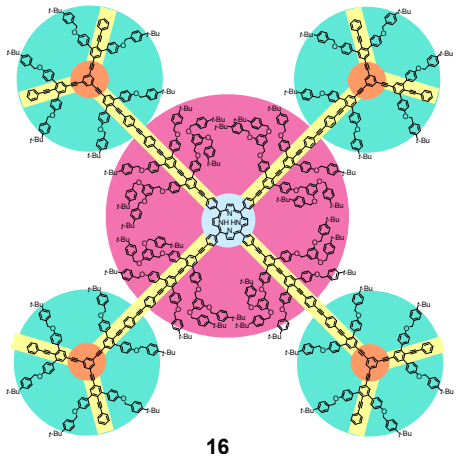

16

$C_{1188}H_{1070}N_4O_{56}$ MW 16,299

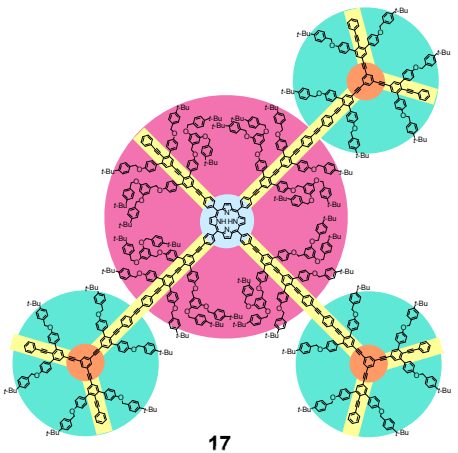

17

$C_{1030}H_{934}N_4O_{50}$MW 14,172

Advantage of Dendrimers in the formation of a nano-scale architecture

- Bonding between the ends of conjugated chain results in the formation of nano-scale architecture with well-defined shape and pai-conjugated network.

Problems in the Assembling Process of Dendrimers

- Low Encounter-probability inhibits an intramolecular reaction. As the results, formation of the product from intramolecular side reaction was increased.
- Separation and purification is problematic. Strong tendency of aggregation impede the GPC-separation.

Separation by GPC

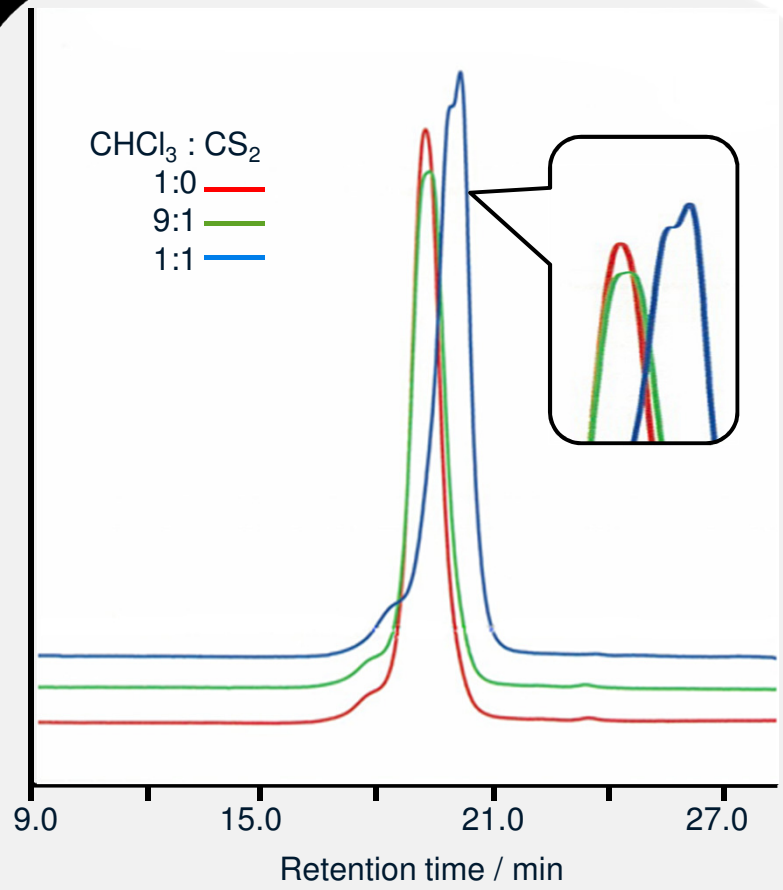

Figure 1. GPC chart of the mixture of **assembly 16** and **17**

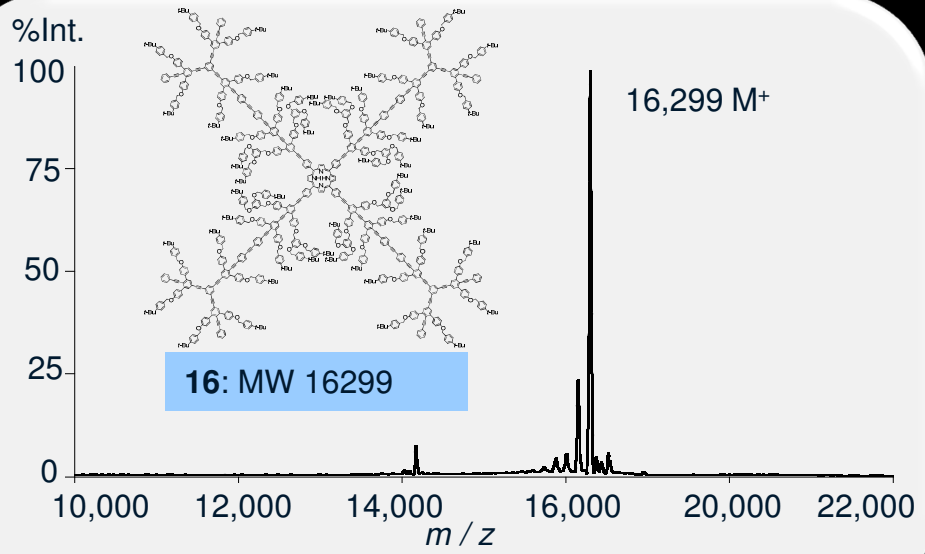

Figure 2. MALDI-TOF MS spectrum of **16**

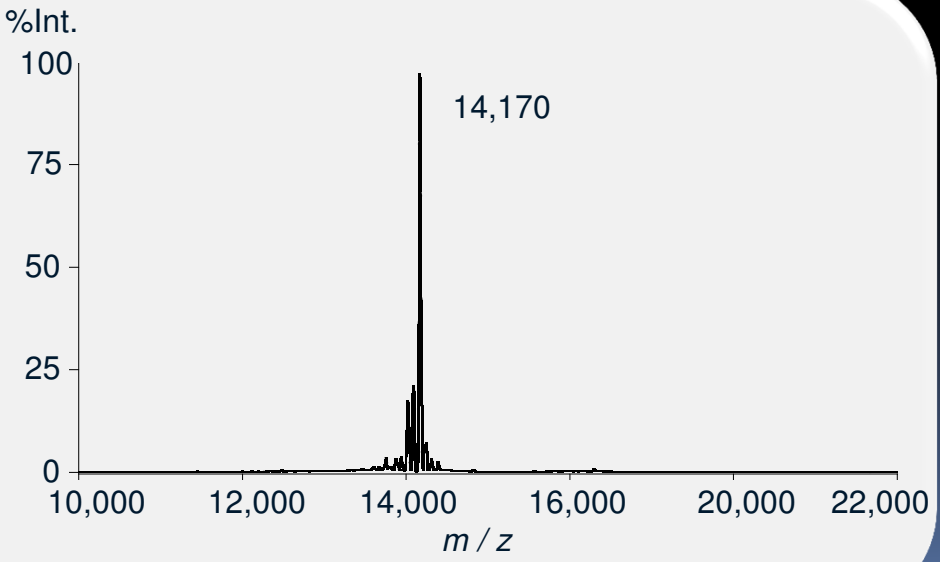

Figure 3. MALDI-TOF MS spectrum of **17**

VT NMR in $CDCl_2CDCl_2$

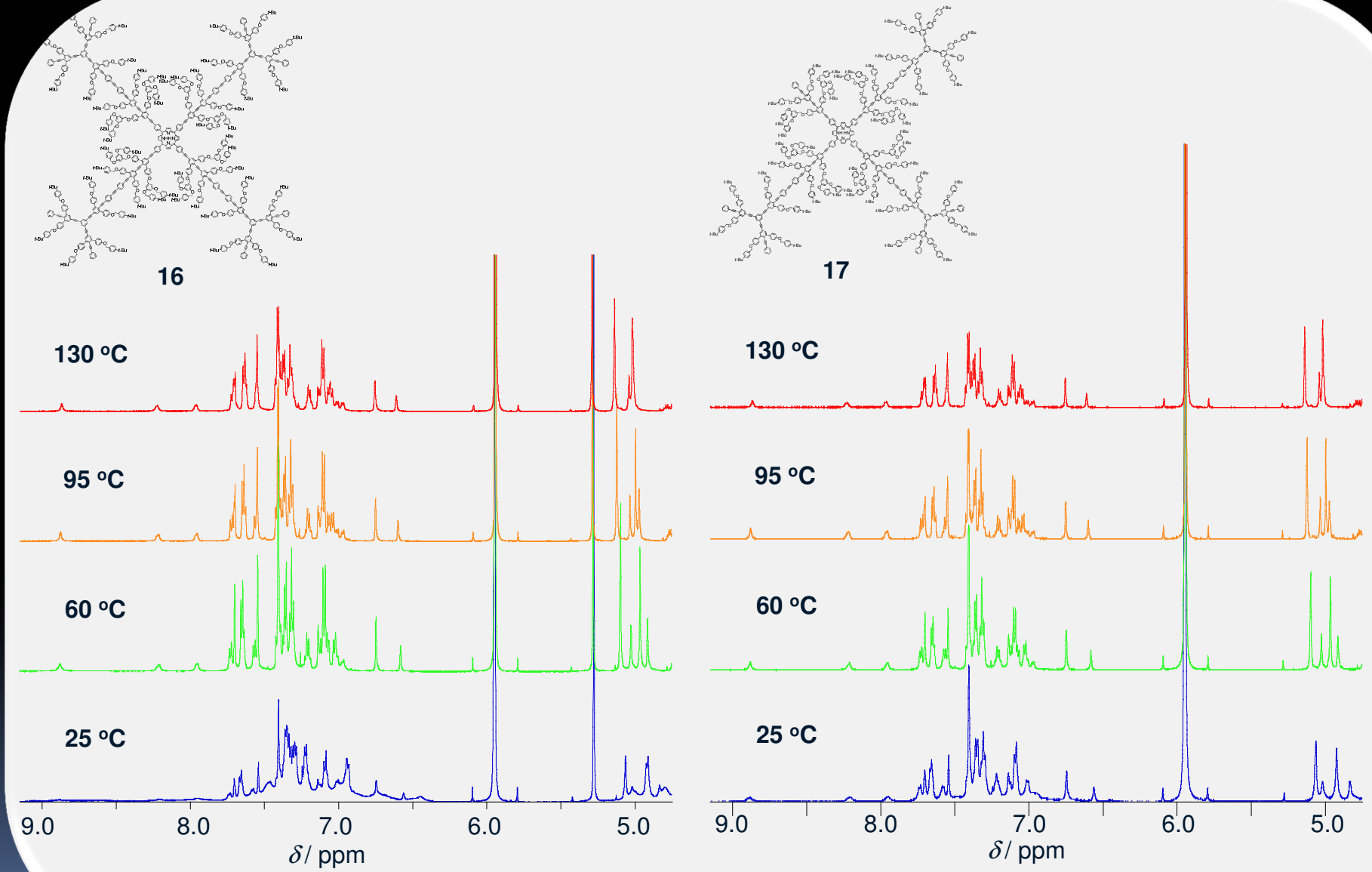

Figure 4. ^{1}H NMR spectra of **16** (left) and **17** (right) in $CDCl_2CDCl_2$ at various temperature

Efficient intramolecular singlet energy transfer

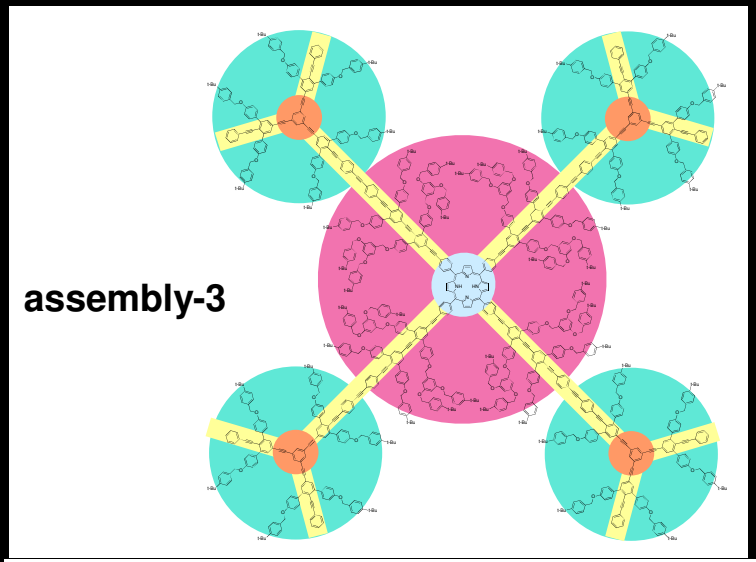

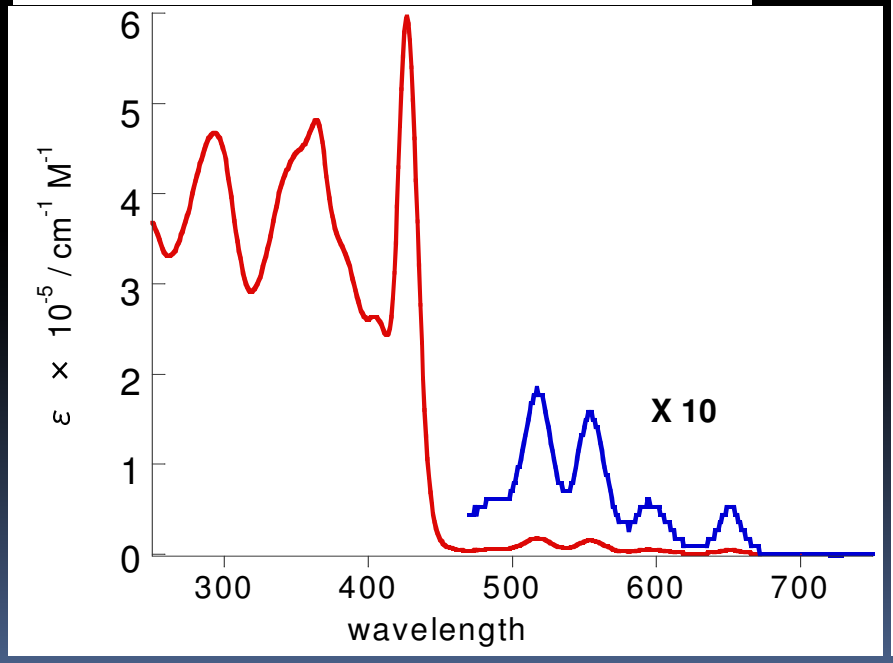

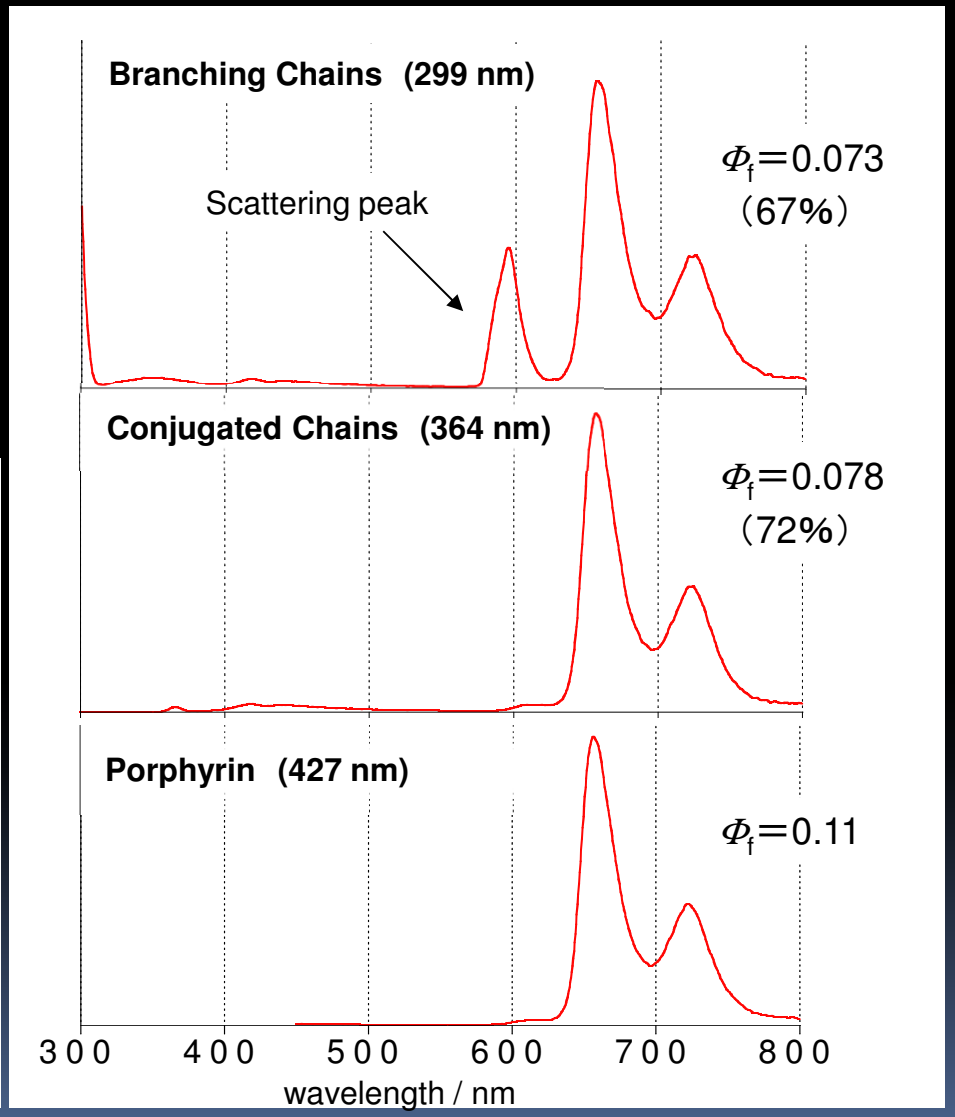

Figure 9. UV-vis spectra of assembly-**3** in THF. (left) Steady-state fluorescence spectra of asesembly-**3** in THF. (right) (a) 286 nm excitation (The intense peak at 598 nm is the scattering of excitation light). (b) 372 nm excitation. (c) 433 nm excitation.

Synthesis of Dendrimers

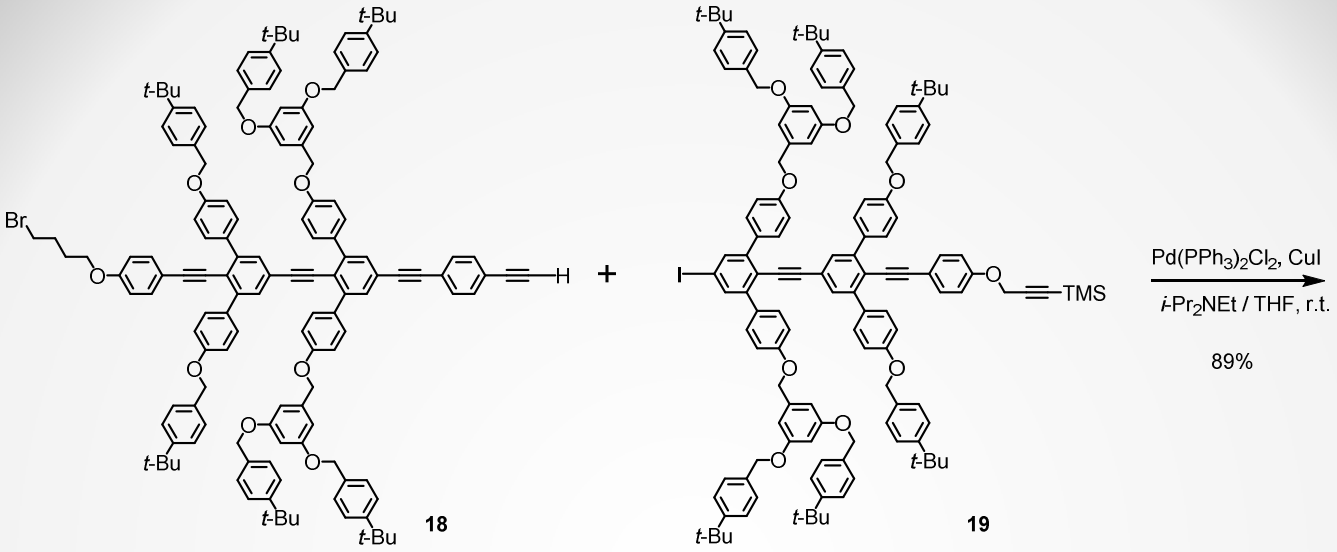

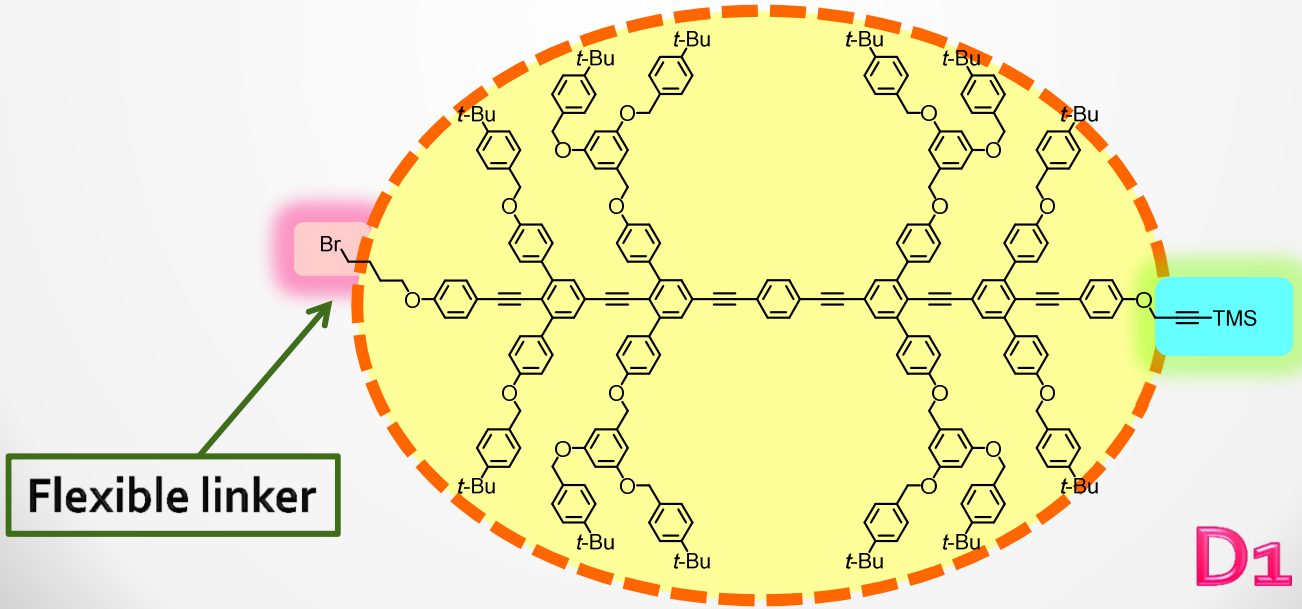

UV-vis Spectra (in CH_2Cl_2)

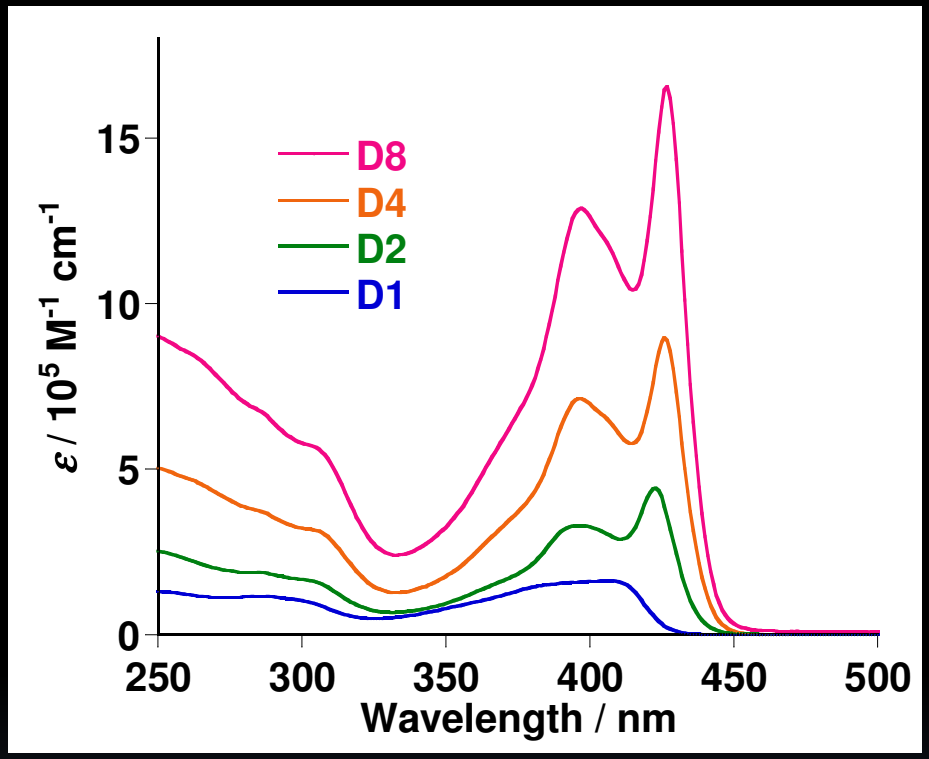

Figure 5. UV-vis spectra of **D1**, **D2**, **D4**, and **D8** in CH_2Cl_2.

	λ_{max} / nm
D1	407
D2	396, 423
D4	397, 426
D8	397, 427

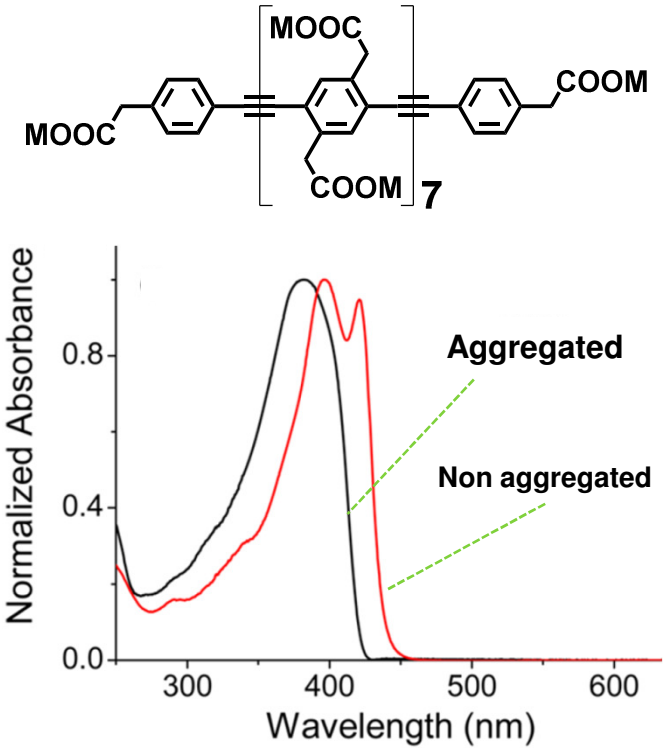

Schanze, K. S. et al.
J. Phys. Chem. Lett. **2013**, *4*, 1410-1414.

Concentration Dependence (in $CHCl_2CHCl_2$)

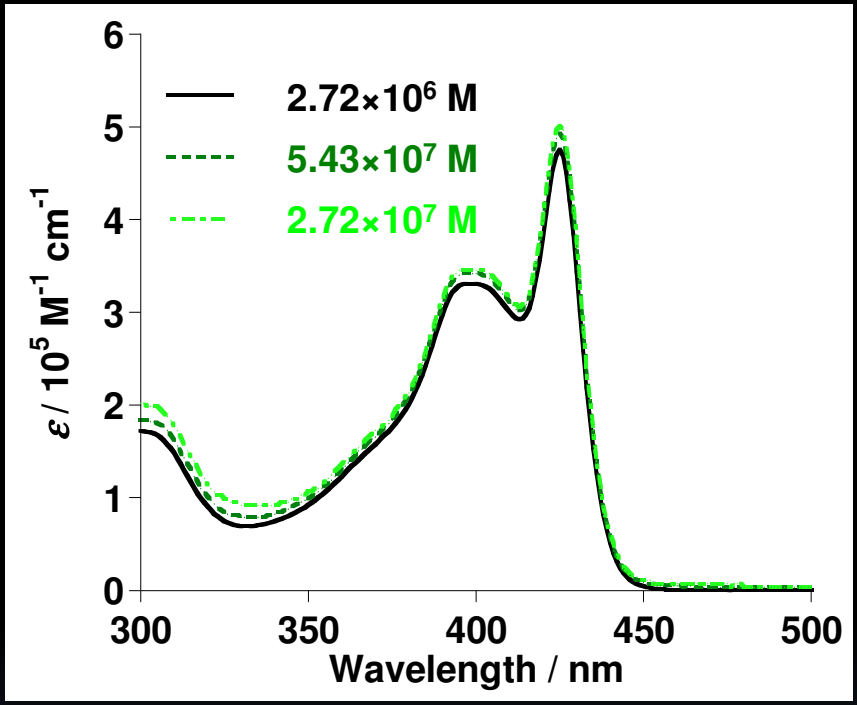

Figure 6. UV-vis spectra of **D2** in $CHCl_2CHCl_2$.

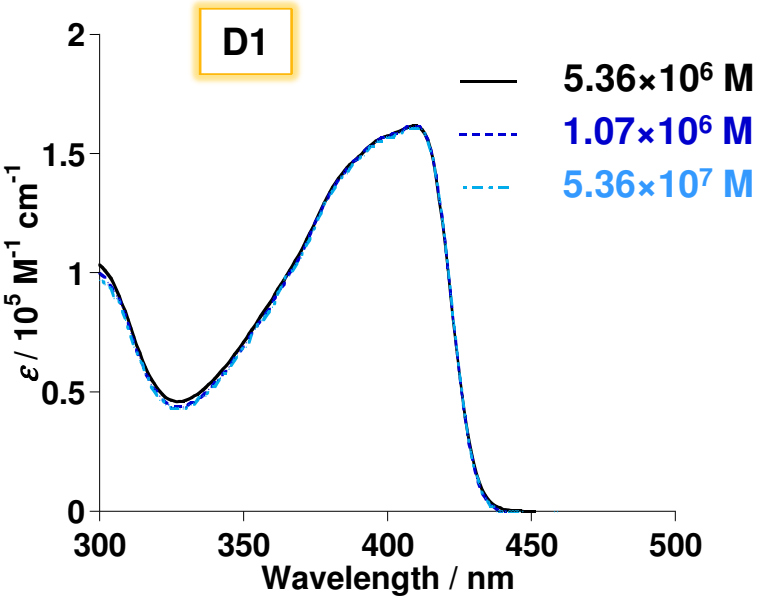

Figure 7. UV-vis spectra of **D1** in $CHCl_2CHCl_2$.

Temperature Dependence (D2 in $CHCl_2CHCl_2$)

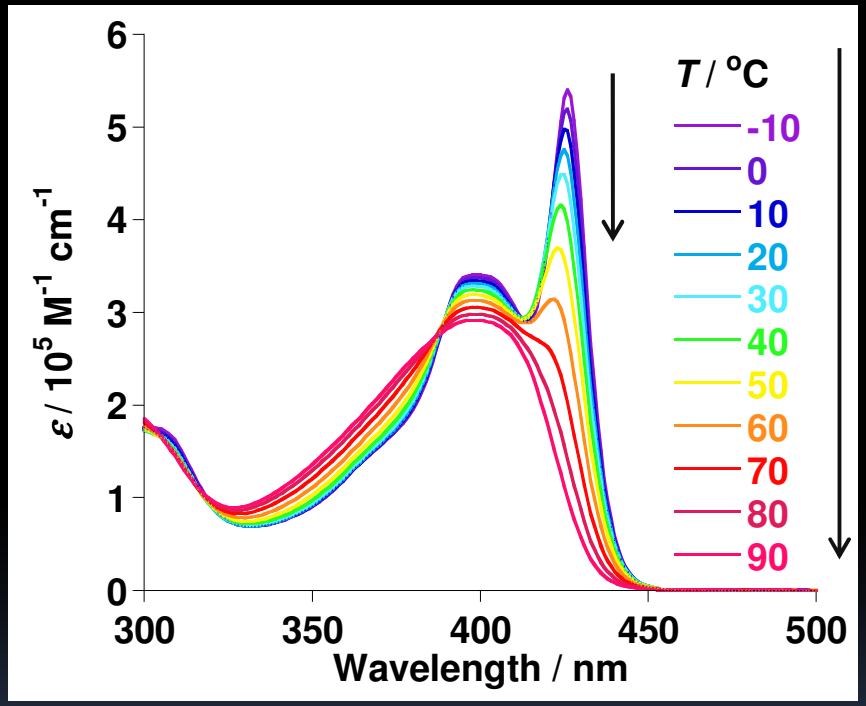

Figure 8. UV-vis spectra of **D2** in $CHCl_2CHCl_2$.

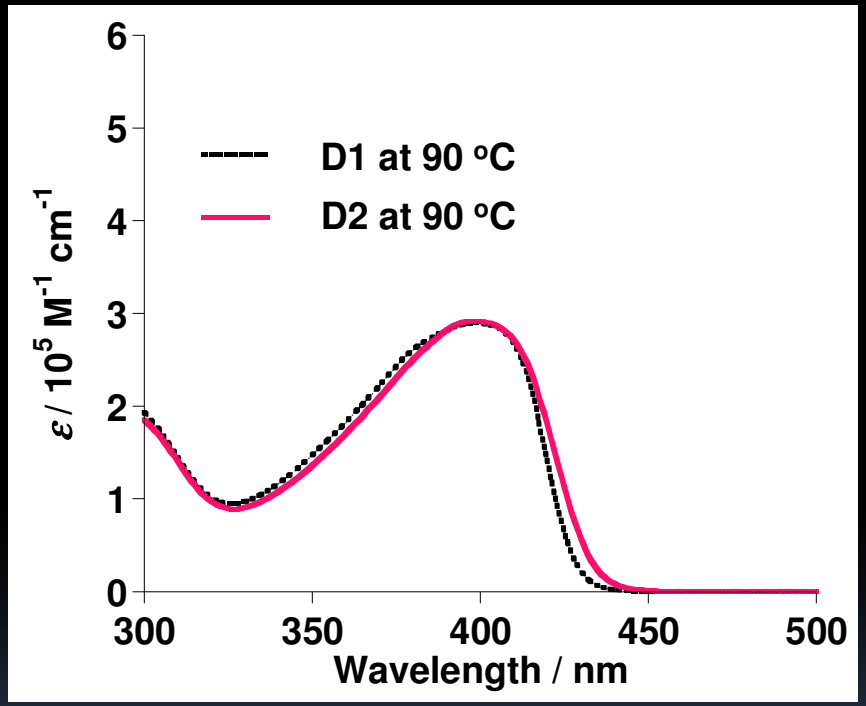

Figure 9. UV-vis spectra of **D1** and **D2** in $CHCl_2CHCl_2$.

Fluorescence Spectra in CH_2Cl_2

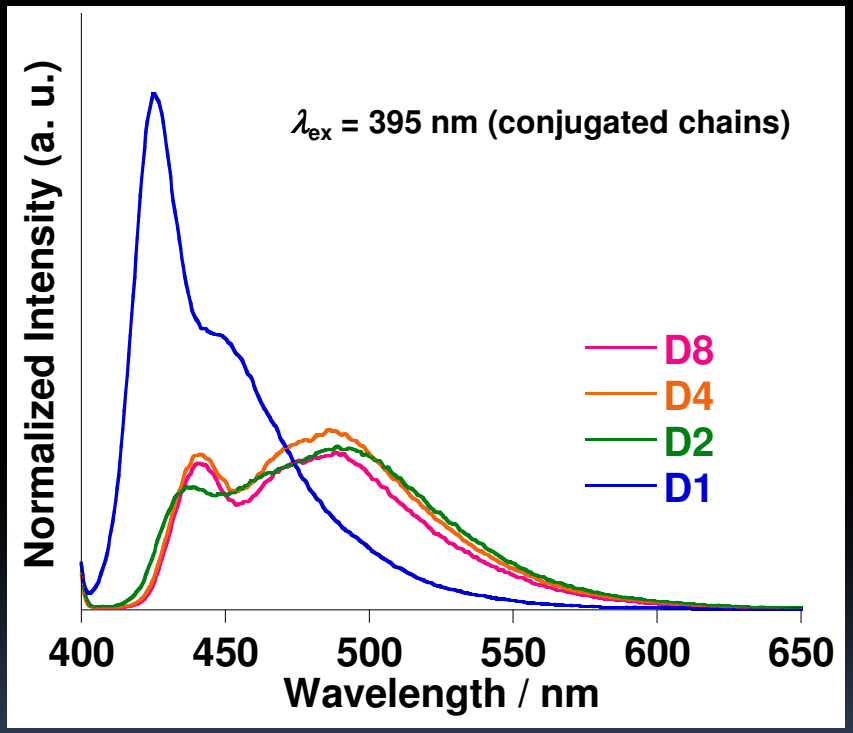

Figure 6. Fluorescence spectra of **D1**, **D2**, **D4**, and **D8** in $CHCl_2CHCl_2$.

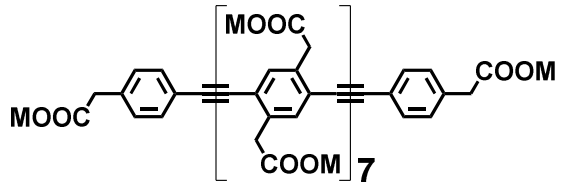

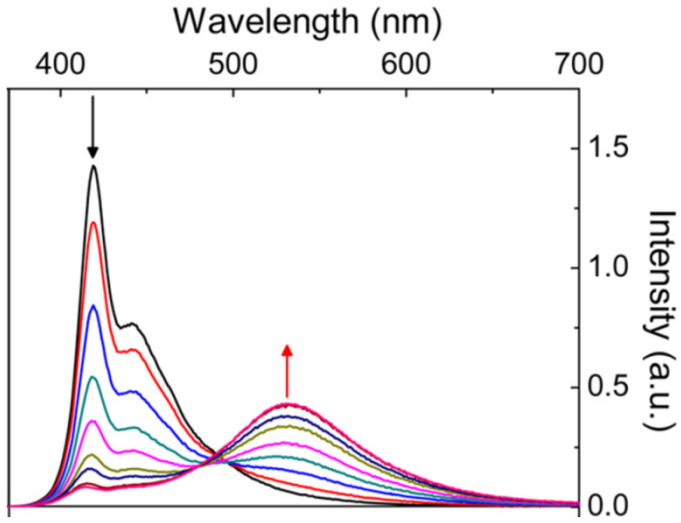

Schanze, K. S. et al.
J. Phys. Chem. Lett. **2013**, *4*, 1410-1414.

Higher Order Structure of Octamer

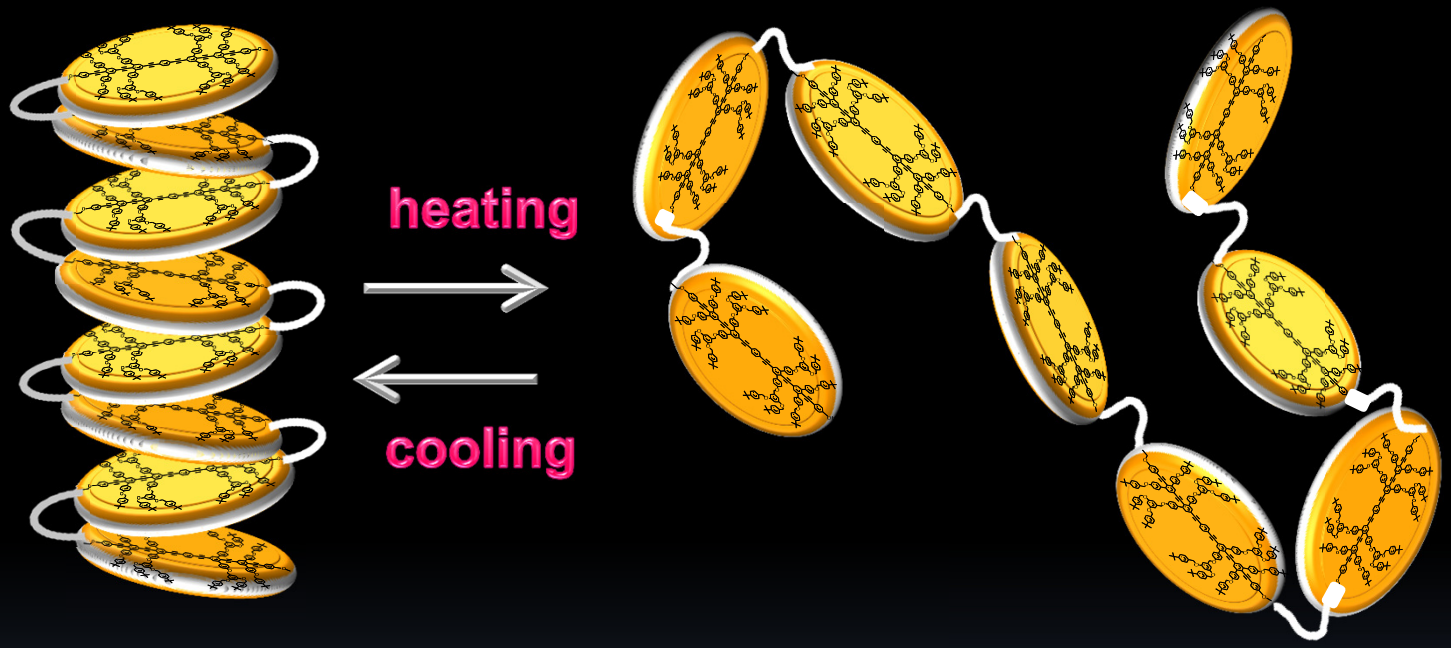

Folded form

Extended form